# Hydrodynamic and Suspended-Solids Concentration Measurements in Suisun Bay, California, 1995

*By* Jay I. Cuetara, Jon R. Burau, *and* David H. Schoellhamer

---

U.S. GEOLOGICAL SURVEY

Water-Resources Investigations Report 01-4086

Prepared in cooperation with the

CALIFORNIA DEPARTMENT OF WATER RESOURCES and the

U.S. BUREAU OF RECLAMATION



Sacramento, California
2001

U.S. DEPARTMENT OF THE INTERIOR
GALE A. NORTON, Secretary

U.S. GEOLOGICAL SURVEY
Charles G. Groat, Director



For additional information write to:

District Chief
U.S. Geological Survey
Placer Hall, Suite 2012
6000 J Street
Sacramento, CA 95819-6129

Copies of this report can be purchased from:

U.S. Geological Survey
Information Services
Box 25286
Federal Center
Denver, CO 80225

# CONTENTS

## FIGURES

## TABLES

## CONVERSION FACTORS, ABBREVIATIONS, ACRONYMS, DATA-COLLECTION STATIONS, SYMBOLS, AND JULIAN DATE CALENDAR

| Multiply | By | To obtain |
|---|---|---|
| centimeter (cm) | 0.3937 | inch |
| centimeter per second (cm/s) | 0.3937 | inch per second |
| cubic meter per second ($m^3/s$) | 35.31 | cubic foot per second |
| decibar (dbar) | 1.0197 | meters of water (at 4°C) |
| kilometer (km) | 0.6214 | mile |
| square kilometer ($km^2$) | 0.3861 | square mile |
| meter (m) | 3.281 | foot |
| meter per second (m/s) | 3.281 | foot per second |
| meter per second squared ($m/s^2$) | 3.281 | foot per second squared |
| millibar (mbar) | 0.0145 | pounds per square inch |
| millimeter (mm) | 0.03937 | inch |
| square meter ($m^2$) | 10.76 | square foot |

Temperature in degrees Celsius (ºC) may be converted to degrees Fahrenheit (ºF) as follows:

$$ºF = (1.8 \times ºC) + 32$$

Abbreviations and Acronyms:

| | |
|---|---|
| deg, | degrees |
| deg. C | degrees Celcius |
| deg. T, | degrees true |
| E | equilibrium argument |
| Hz | hertz |
| kHz, | kilohertz |
| mg/L | milligram per liter |
| mS/CM, mS/cm, | millisiemens per centimeter |
| mmhos/cm, | millimhos per centimeter |
| μm | micrometer |
| μS/cm | microsiemens per centimeter |
| ppt, | parts per thousand |
| cfs, | cubic feet per second |
| cms, | cubic meter per second |
| ADCP, | Acoustic Doppler Current Profiler |
| BIN, | a depth cell from an ADCP |
| CT, | conductivity-temperature |
| CTD, | conductivity-temperature-depth |
| CTDO, | conductivity-temperature-depth-optical backscatter |
| DAYFLOW, | California Department of Water Resources delta outflow |
| DWR, | California Department of Water Resources |
| ETM, | estuarine turbidity maximum |
| EZ, | entrapment zone |
| FTU, | formazine turbidity unit |
| IEP, | Interagency Ecological Program for the San Francisco Bay Estuary |
| MLLW, | mean lower low water |
| OBS | optical backscatteranced sensor |
| RDI | R.D. Instruments, Inc. |
| RMS, | root-mean-squared |
| SC, | specific conductance |
| SI | (System International) International System of Weights and Measures |
| SSC | suspended-solids concentration |
| SSF | suspended-solids flux |
| UNESCO | United Nations Educational, Scientific, and Cultural Organization |
| USBR, | U.S. Bureau of Reclamation |
| USGS, | U.S. Geological Survey |

Data-collection stations:

| | | | | | | | |
|---|---|---|---|---|---|---|---|
| BEN | BULLS | CARQ | MET | CUT | GARN | GARNW | |
| GC | GDOL | GS | HC | HDOL | HS | MAL | MART |
| MID | MOTH | RYER | RYERE | SPOON | WICK | | |

Tidal symbols:

| | | | | | | | | | |
|---|---|---|---|---|---|---|---|---|---|
| $J_1$ | $K_1$ | $K_2$ | $L_2$ | $M_1$ | $M_2$ | $M_4$ | $Mk_3$ | $Mu_2$ | $\mu_2$ |
| $m_2$ | $N_2$ | $Nu_2$ | $n_2$ | $O_1$ | $P_1$ | $Q_1$ | $S_2$ | $T_2$ | $v_2$ |

## Vertical Datum

*Sea level*: In this report, “sea level” refers to the National Geodetic Vertical Datum of 1929 (NGVD of 1929), a geodetic datum derived from a general adjustment of the first-order level nets of both the United States and Canada, formerly called Sea Level Datum of 1929.

All depths in this report are referenced to mean lower low water (MLLW). For the purpose of this report, the difference between MLLW and sea level is assumed to be 1.0 m within Suisun Bay.

Salinities in this report are presented without (practical salinity) units because salinity is a conductivity ratio; therefore, it has no physical units.

# Julian Date Calendar

| For nonleap years | | | | | | | | | | | | | | |
|---|---|---|---|---|---|---|---|---|---|---|---|---|---|---|
| **Day** | **Dec** | **Jan** | **Feb** | **Mar** | **Apr** | **May** | **June** | **July** | **Aug** | **Sept** | **Oct** | **Nov** | **Dec** | **Day** |
| 1 | -30 | 1 | 32 | 60 | 91 | 121 | 152 | 182 | 213 | 244 | 274 | 305 | 335 | 1 |
| 2 | -29 | 2 | 33 | 61 | 92 | 122 | 153 | 183 | 214 | 245 | 275 | 306 | 336 | 2 |
| 3 | -28 | 3 | 34 | 62 | 93 | 123 | 154 | 184 | 215 | 246 | 276 | 307 | 337 | 3 |
| 4 | -27 | 4 | 35 | 63 | 94 | 124 | 155 | 185 | 216 | 247 | 277 | 308 | 338 | 4 |
| 5 | -26 | 5 | 36 | 64 | 95 | 125 | 156 | 186 | 217 | 248 | 278 | 309 | 339 | 5 |
| 6 | -25 | 6 | 37 | 65 | 96 | 126 | 157 | 187 | 218 | 249 | 279 | 310 | 340 | 6 |
| 7 | -24 | 7 | 38 | 66 | 97 | 127 | 158 | 188 | 219 | 250 | 280 | 311 | 341 | 7 |
| 8 | -23 | 8 | 39 | 67 | 98 | 128 | 159 | 189 | 220 | 251 | 281 | 312 | 342 | 8 |
| 9 | -22 | 9 | 40 | 68 | 99 | 129 | 160 | 190 | 221 | 252 | 282 | 313 | 343 | 9 |
| 10 | -21 | 10 | 41 | 69 | 100 | 130 | 161 | 191 | 222 | 253 | 283 | 314 | 344 | 10 |
| 11 | -20 | 11 | 42 | 70 | 101 | 131 | 162 | 192 | 223 | 254 | 284 | 315 | 345 | 11 |
| 12 | -19 | 12 | 43 | 71 | 102 | 132 | 163 | 193 | 224 | 255 | 285 | 316 | 346 | 12 |
| 13 | -18 | 13 | 44 | 72 | 103 | 133 | 164 | 194 | 225 | 256 | 286 | 317 | 347 | 13 |
| 14 | -17 | 14 | 45 | 73 | 104 | 134 | 165 | 195 | 226 | 257 | 287 | 318 | 348 | 14 |
| 15 | -16 | 15 | 46 | 74 | 105 | 135 | 166 | 196 | 227 | 258 | 288 | 319 | 349 | 15 |
| 16 | -15 | 16 | 47 | 75 | 106 | 136 | 167 | 197 | 228 | 259 | 289 | 320 | 350 | 16 |
| 17 | -14 | 17 | 48 | 76 | 107 | 137 | 168 | 198 | 229 | 260 | 290 | 321 | 351 | 17 |
| 18 | -13 | 18 | 49 | 77 | 108 | 138 | 169 | 199 | 230 | 261 | 291 | 322 | 352 | 18 |
| 19 | -12 | 19 | 50 | 78 | 109 | 139 | 170 | 200 | 231 | 262 | 292 | 323 | 353 | 19 |
| 20 | -11 | 20 | 51 | 79 | 110 | 140 | 171 | 201 | 232 | 263 | 293 | 324 | 354 | 20 |
| 21 | -10 | 21 | 52 | 80 | 111 | 141 | 172 | 202 | 233 | 264 | 294 | 325 | 355 | 21 |
| 22 | -9 | 22 | 53 | 81 | 112 | 142 | 173 | 203 | 234 | 265 | 295 | 326 | 356 | 22 |
| 23 | -8 | 23 | 54 | 82 | 113 | 143 | 174 | 204 | 235 | 266 | 296 | 327 | 357 | 23 |
| 24 | -7 | 24 | 55 | 83 | 114 | 144 | 175 | 205 | 236 | 267 | 297 | 328 | 358 | 24 |
| 25 | -6 | 25 | 56 | 84 | 115 | 145 | 176 | 206 | 237 | 268 | 298 | 329 | 359 | 25 |
| 26 | -5 | 26 | 57 | 85 | 116 | 146 | 177 | 207 | 238 | 269 | 299 | 330 | 360 | 26 |
| 27 | -4 | 27 | 58 | 86 | 117 | 147 | 178 | 208 | 239 | 270 | 300 | 331 | 361 | 27 |
| 28 | -3 | 28 | 59 | 87 | 118 | 148 | 179 | 209 | 240 | 271 | 301 | 332 | 362 | 28 |
| 29 | -2 | 29 | | 88 | 119 | 149 | 180 | 210 | 241 | 272 | 302 | 333 | 363 | 29 |
| 30 | -1 | 30 | | 89 | 120 | 150 | 181 | 211 | 242 | 273 | 303 | 334 | 364 | 30 |
| 31 | | 31 | | 90 | | 151 | | 212 | 243 | | 304 | | 365 | 31 |

# Julian Date Calendar—Continued

**For leap years**

| Day | Dec | Jan | Feb | Mar | Apr | May | June | July | Aug | Sept | Oct | Nov | Dec | Day |
|---|---|---|---|---|---|---|---|---|---|---|---|---|---|---|
| 1 | -30 | 1 | 32 | 61 | 92 | 122 | 153 | 183 | 214 | 245 | 275 | 306 | 336 | 1 |
| 2 | -29 | 2 | 33 | 62 | 93 | 123 | 154 | 184 | 215 | 246 | 276 | 307 | 337 | 2 |
| 3 | -28 | 3 | 34 | 63 | 94 | 124 | 155 | 185 | 216 | 247 | 277 | 308 | 338 | 3 |
| 4 | -27 | 4 | 35 | 64 | 95 | 125 | 156 | 186 | 217 | 248 | 278 | 309 | 339 | 4 |
| 5 | -26 | 5 | 36 | 65 | 96 | 126 | 157 | 187 | 218 | 249 | 279 | 310 | 340 | 5 |
| 6 | -25 | 6 | 37 | 66 | 97 | 127 | 158 | 188 | 219 | 250 | 280 | 311 | 341 | 6 |
| 7 | -24 | 7 | 38 | 67 | 98 | 128 | 159 | 189 | 220 | 251 | 281 | 312 | 342 | 7 |
| 8 | -23 | 8 | 39 | 68 | 99 | 129 | 160 | 190 | 221 | 252 | 282 | 313 | 343 | 8 |
| 9 | -22 | 9 | 40 | 69 | 100 | 130 | 161 | 191 | 222 | 253 | 283 | 314 | 344 | 9 |
| 10 | -21 | 10 | 41 | 70 | 101 | 131 | 162 | 192 | 223 | 254 | 284 | 315 | 345 | 10 |
| 11 | -20 | 11 | 42 | 71 | 102 | 132 | 163 | 193 | 224 | 255 | 285 | 316 | 346 | 11 |
| 12 | -19 | 12 | 43 | 72 | 103 | 133 | 164 | 194 | 225 | 256 | 286 | 317 | 347 | 12 |
| 13 | -18 | 13 | 44 | 73 | 104 | 134 | 165 | 195 | 226 | 257 | 287 | 318 | 348 | 13 |
| 14 | -17 | 14 | 45 | 74 | 105 | 135 | 166 | 196 | 227 | 258 | 288 | 319 | 349 | 14 |
| 15 | -16 | 15 | 46 | 75 | 106 | 136 | 167 | 197 | 228 | 259 | 289 | 320 | 350 | 15 |
| 16 | -15 | 16 | 47 | 76 | 107 | 137 | 168 | 198 | 229 | 260 | 290 | 321 | 351 | 16 |
| 17 | -14 | 17 | 48 | 77 | 108 | 138 | 169 | 199 | 230 | 261 | 291 | 322 | 352 | 17 |
| 18 | -13 | 18 | 49 | 78 | 109 | 139 | 170 | 200 | 231 | 262 | 292 | 323 | 353 | 18 |
| 19 | -12 | 19 | 50 | 79 | 110 | 140 | 171 | 201 | 232 | 263 | 293 | 324 | 354 | 19 |
| 20 | -11 | 20 | 51 | 80 | 111 | 141 | 172 | 202 | 233 | 264 | 294 | 325 | 355 | 20 |
| 21 | -10 | 21 | 52 | 81 | 112 | 142 | 173 | 203 | 234 | 265 | 295 | 326 | 356 | 21 |
| 22 | -9 | 22 | 53 | 82 | 113 | 143 | 174 | 204 | 235 | 266 | 296 | 327 | 357 | 22 |
| 23 | -8 | 23 | 54 | 83 | 114 | 144 | 175 | 205 | 236 | 267 | 297 | 328 | 358 | 23 |
| 24 | -7 | 24 | 55 | 84 | 115 | 145 | 176 | 206 | 237 | 268 | 298 | 329 | 359 | 24 |
| 25 | -6 | 25 | 56 | 85 | 116 | 146 | 177 | 207 | 238 | 269 | 299 | 330 | 360 | 25 |
| 26 | -5 | 26 | 57 | 86 | 117 | 147 | 178 | 208 | 239 | 270 | 300 | 331 | 361 | 26 |
| 27 | -4 | 27 | 58 | 87 | 118 | 148 | 179 | 209 | 240 | 271 | 301 | 332 | 362 | 27 |
| 28 | -3 | 28 | 59 | 88 | 119 | 149 | 180 | 210 | 241 | 272 | 302 | 333 | 363 | 28 |
| 29 | -2 | 29 | 60 | 89 | 120 | 150 | 181 | 211 | 242 | 273 | 303 | 334 | 364 | 29 |
| 30 | -1 | 30 | | 90 | 121 | 151 | 182 | 212 | 243 | 274 | 304 | 335 | 365 | 30 |
| 31 | | 31 | | 91 | | 152 | | 213 | 244 | | 305 | | 366 | 31 |

# Hydrodynamic and Suspended-Solids Concentration Measurements in Suisun Bay, California, 1995

*By* Jay I. Cuetara, Jon R. Burau, *and* David H. Schoellhamer

## ABSTRACT

Sea level, current velocity, water temperature, salinity (computed from conductivity and temperature), and suspended-solids data collected in Suisun Bay, California, from May 30, 1995, through October 27, 1995, by the U.S. Geological Survey are documented in this report. Data were collected concurrently at 21 sites. Various parameters were measured at each site. Velocity-profile data were collected at 6 sites, single-point velocity measurements were made at 9 sites, salinity data were collected at 20 sites, and suspended-solids concentrations were measured at 10 sites. Sea-level and velocity data are presented in three forms; harmonic analysis results; time-series plots (sea level, current speed, and current direction versus time); and time-series plots of low-pass-filtered time series. Temperature, salinity, and suspended-solids data are presented as plots of raw and low-pass-filtered time series.

The velocity and salinity data presented in this report document a period when the residual current patterns and salt field were transitioning from a freshwater-inflow-dominated condition towards a quasi steady-state summer condition when density-driven circulation and tidal nonlinearities became relatively more important as long-term transport mechanisms. Sacramento–San Joaquin River Delta outflow was high prior to and during this study, so the tidally averaged salinities were abnormally low for this time of year. For example, the tidally averaged salinities varied from 0–12 at Martinez, the western border of Suisun Bay, to a maximum of 2 at Mallard Island, the eastern border of Suisun Bay.

Even though salinities increased overall in Suisun Bay during the study period, the near-bed residual currents primarily were directed seaward. Therefore, salinity intrusion through Suisun Bay towards the Delta primarily was accomplished in the absence of the tidally averaged, two-layer flow known as gravitational circulation where, by definition, the net currents are landward at the bed. The Folsom Dam spillway gate failure on July 17, 1995, was analyzed to determine the effect on the hydrodynamics of Suisun Bay. The peak flow of the American River reached roughly 1,000 cubic meters per second as a result of the failure, which is relatively small. This was roughly 15 percent of the approximate 7,000 cubic meters per second tidal flows that occur daily in Suisun Bay and was likely attenuated greatly. Based on analysis of tidally averaged near-bed salinity and depth-averaged currents after the failure, the effect was essentially nonexistent and is indistinguishable from the natural variability.

## INTRODUCTION

The data described in this report were collected in cooperation with the California Department of Water Resources (DWR) and the U.S. Bureau of Reclamation (USBR) as part of ongoing research by the U.S. Geological Survey (USGS) into the hydrodynamics of the San Francisco Bay estuary (fig. 1). These

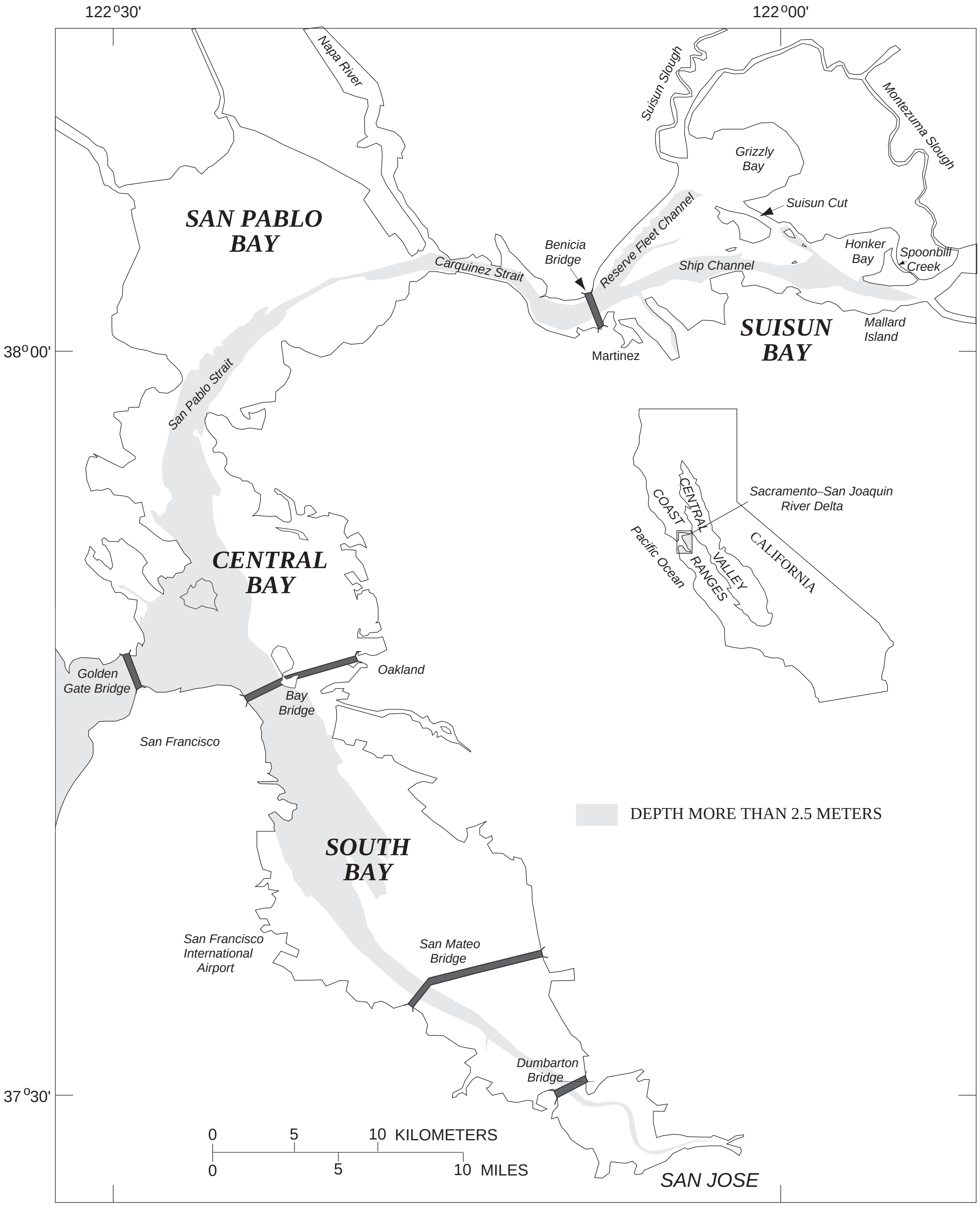


**Figure 1.** San Francisco Bay Estuary, California.

data were collected as part of the Interagency Ecological Program (IEP) sponsored interdisciplinary entrapment zone (EZ) study (Kimmerer, 1998) and USGS Place-Based Program. Other agencies involved in the IEP include the California Department of Fish and Game and the U.S. Fish and Wildlife Service. The USGS conducts a wide range of research and monitoring activities in the San Francisco Bay estuary (Cloern and others, 1995). Research includes many disciplines, including climate change (Peterson and others, 1995), hydrodynamics (Smith and others, 1995), sediment transport (Schoellhamer and others, 1997), phytoplankton dynamics (Cloern and Jassby, 1995), toxic contamination (Luoma and others, 1993; Kuivila and Foe, 1995), and exotic species (Nichols and others, 1990). For an updated list of USGS publications, see the Access USGS web site at http://sfbay.wr.usgs.gov/access/pubs.html.

## Purpose and Scope

This report documents hydrodynamic and suspended-solids concentration (SSC) data collected in Suisun Bay (fig. 1) from May 30, 1995, through October 27, 1995, through plots and harmonic analysis results. Five distinct types of data were collected and analyzed; (1) sea-level data measured with a pressure sensor at depth or a surface float; (2) velocity data consisting of magnitude and direction, either at a single point or equally spaced points in the vertical, depending on the depth at each location; (3) water-temperature data, (4) salinity data calculated from measured values of conductivity and temperature; and (5) suspended-solids data collected with optical backscatterance sensors (OBS). Additionally, hydrologic and meteorological data are presented. The hydrologic data consists of the Sacramento–San Joaquin Delta outflow, and the meteorological data include measured values of barometric pressure, wind speed and direction, air temperature, and visible light.

The principal objective for collecting these data was to measure the spatial and temporal variability in the residual currents, salinity, and SSC in the channels of Suisun Bay. Acoustic Doppler current profilers (ADCPs) were deployed in the channels to vertically define the velocity structure. In order to estimate salinity and sediment fluxes, conductivity-temperature-depth-optical backscatterance (CTDO) sensors were deployed adjacent to the velocity measuring instruments, where possible. Station locations are shown in figure 2; their respective latitudes, longitudes, and deployment dates are given in table 1. The instrument specifications are presented in table 2.

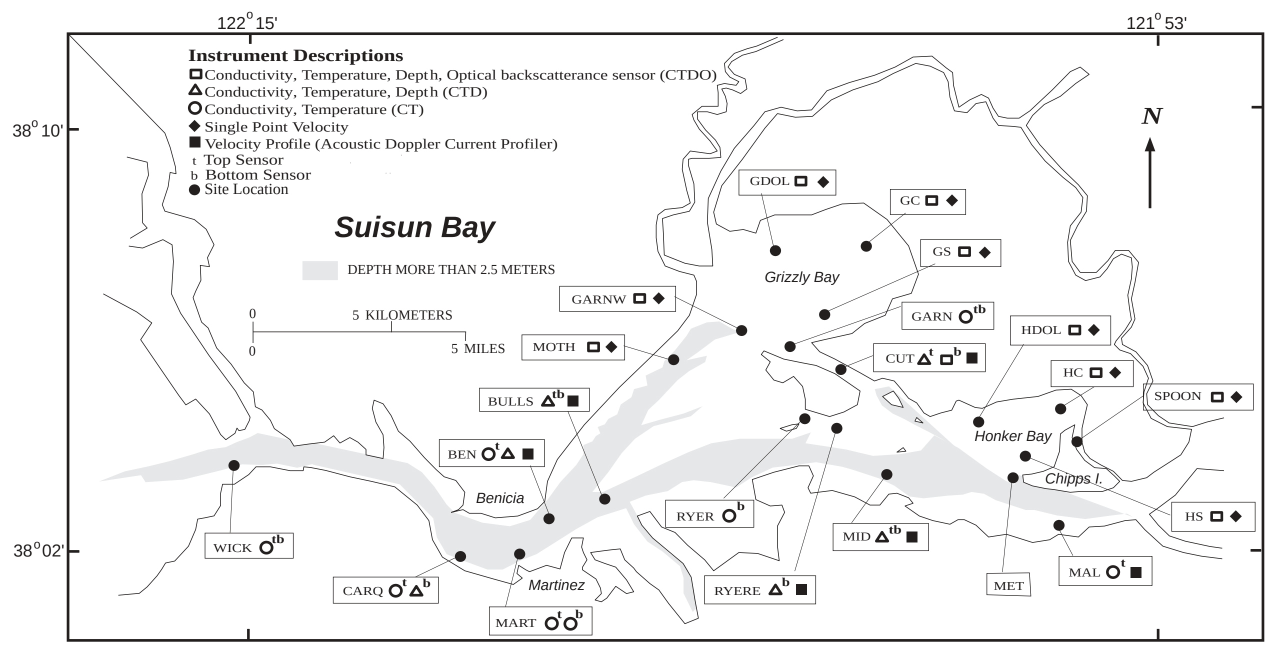


**Figure 2.** Data-collection locations and station names, Suisun Bay, California.

**Table 1.** Data-collection instrument locations and deployment periods

[MLLW, mean lower low water; m, meters; na, not applicable; v, velocity sensor; s, salinity sensor; p, pressure sensor or sea level sensor; o, optical backscatterance sensor; nb, narrow-band acoustic Doppler current profiler; bb, broad-band acoustic Doppler current profiler]

| Station Name | Position | Depth (MLLW In meters) | Sensor depth (meters) | Deployment period (Julian Days) |
|---|---|---|---|---|
| BEN (nb, s, p) | 38°02′37″ 122°07′25″ | 18.6 m | +2.1 m, +10.0 m, and +17.7 m | 5/20/95 (140) – 10/31/95 (304) |
| BULLS (bb, s, p) | 38°02′54″ 122°06′01″ | 12.3 m | +5.5 m and +11.5 m | 6/01/95 (152) – 10/23/9 5(296) |
| CARQ (s, p) | 38°02′35″ 122°10′31″ | 17.5 m | +9.3 m and +17.0 m | 6/05/95 (156) – 11/01/95 (305) |
| CUT (nb, s, p, o) | 38°05′24″ 122°00′20″ | 8.3 m | +3.1 m and +7.5 m | 7/07/95 (188) – 10/23/95 (296) |
| GARN (s) | 38°05′44″ 122°01′32″ | 6.1 m | +1.4 m and +5.3 m | 7/05/95 (186) – 10/22/95 (295) |
| GARNW (v, s, p, o) | 38°06′23″ 122°02′53″ | 2.4 m | +1.8 m (v) and +1.7 m | 9/18/95 (261) – 10/23/95 (296) |
| GC (v, s, p, o) | 38°07′12″ 122°01′34″ | 1.4 m | +0.8 m (v) and +0.7 m | 7/04/95 (185) – 8/18/95 (230) |
| GDOL (v, s, p, o) | 38°07′01″ 122°02′26″ | 1.7 m | +1.1 m (v) and +1.0 m | 7/06/95 (187) – 9/18/95 (261) |
| GS (v, s, p, o) | 38°06′28″ 122°01′22″ | 1.2 m | +0.6 m (v) and +0.5 m | 7/06/95 (187) – 9/18/95 (261) |
| HC (v, s, p, o) | 38°04′26″ 121°55′45″ | 0.9 m | +0.3 m (v) and +0.2 m | 7/09/95 (190) – 10/24/95 (297) |
| HDOL (v, s, p, o) | 38°04′25″ 121°57′27″ | 1.9 m | +1.5 m (v) and +1.5 m | 7/06/95 (187) – 9/18/95 (261) |
| HS (v, s, p, o) | 38°03′28″ 121°55′59″ | 1.1 m | +0.5 m (v) and +0.4 m | 7/07/95 (188) – 9/18/95 (261) |
| MAL (bb, s, p) | 38°02′33″ 121°54′59″ | 16.4 m | +15.4 m | 5/30/95 (150) – 10/27/95 (300) |
| MART (s, p) | 38°01′40″ 122°08′22″ | 8.0 m | +1.0 m and +7.5 m | 7/06/95 (187) – 11/16/95 (320) |
| MET | 38°03′10″ 121°56′10″ | na | na | 5/01/95 (121) – 11/01/95 (305) |

**Table 1.** Data-collection instrument locations and deployment periods—Continued

| Station Name | Position | Depth (MLLW In meters) | Sensor depth (meters) | Deployment period (Julian Days) |
|---|---|---|---|---|
| MID (bb, s, p) | 38°03′42″<br>122°00′03″ | 8.5 m | +0.8 m and +7.7 m | 6/01/95 (152) –<br>10/23/95 (296) |
| MOTH (v, s, p, o) | 38°05′29″<br>122°04′30″ | 8.9 m | +8.3 m (v) and +8.2 m | 9/18/95 (261) –<br>10/23/95 (296) |
| RYER (s) | 38°04′45″<br>122°02′11″ | 6.2 m | +5.4 m | 7/07/95 (188) –<br>8/18/95 (230) |
| RYERE (nb, s, p) | 38°04′28″<br>122°01′16″ | 5.3 m | +4.5 m | 6/01/95 (152) –<br>8/18/95 (230) |
| SPOON (v, s, p, o) | 38°04′15″<br>121°54′42″ | 2.4 m | +1.5 m (v) and +1.6 m | 9/18/95 (261) –<br>10/24/95 (297) |
| WICK (s) | 38°03′30″<br>122°14′24″ | 15.3 m | +0.3 m and +12.6 m | 4/30/95 (120) –<br>10/31/95 (304) |

**Table 2.** Specifications for instruments used in Suisun Bay, California

[Salinities in this report are presented in practical salinity units, which is a conductivity ratio; therefore, it has no physical units (Millero, 1993); °C, degrees Celsius; m, meter; mS/cm, millisiemens per centimeter at 25°C; mm, millimdter; dbar, decibar; cm/s, centimeters per second; FS, full scale; CT, conductivity-temperature; CTD, conductivity-temperature-depth sensor; OBS, optical backscatternce sensor; ADCP, acoustic Doppler current profiler; FTU, formazin turbidity unit]

| | Range | Accuracy | Resolution |
|---|---|---|---|
| **Seabird: Seacat CT** | | | |
| Temperature | –5–35ºC | +/- 0.01 | +/- 0.001 |
| Conductivity | 0–70 mS/cm | +/- 0.001 | +/- 0.0001 |
| **Ocean Sensors: Os200 CTD** | | | |
| Temperature | –2– 35ºC | 0.01 percent FS | 0.001 percent FS |
| Conductivity | 0.5–65 mS/cm | 0.02 percent FS | 0.001 percent |
| Salinity | 1–45 | 0.03 percent FS | 0.001 percent |
| Pressure | 0–50 dbar | 0.50 percent FS | 0.005 percent |
| **D & A: Optical Backscatterance Sensor (OBS-3)** | | | |
| Turbidity | 0.02–2,000 FTU | 2.0 percent FS | 0.001 FTU |
| **Interocean Systems: S4 Current Meter** | | | |
| Current Speed | 0–350 cm/s | 2.0 percent FS | 0.2 cm/s |
| Direction | 0–360 degrees | +/- 2 degrees | 0.5 degrees |
| Pressure | 0–70 m | +/- 0.15 percent | 4 mm |
| **EG & G: Velocity Meter** | | | |
| Temperature | –2–35ºC | 0.05ºC | 0.01ºC |
| Pressure | 0–999.9 dbar | 0.5 percent | 0.2 dbar |
| Velocity | 0–360 cm/s | 3 percent | 0.1 cm/s |
| Heading | 0–360 degrees | +/- 5.0 degrees | 1.0 degrees |
| **RD Instruments ADCP: Broad Band and Narrow Band** | | | |
| Velocity | +/- 1,000 cm/s | < 1 cm/s | 0.1 cm/s |
| Heading | 0–360 degrees | 2 degrees | 02 degrees |

The data in this report are organized by location (fig. 2) and primarily presented as time-series plots. Harmonic analysis results characterize the tidal motions, and low-pass-filtered data characterize the residual (tidally averaged) motions. Additional characteristics of the tidal velocities, such as the root-mean-square (RMS) speed, tidal form number, principal current direction, and spring-tide maximum and neap-tide minimum velocities also are presented.

## Study Area

### Geographic Setting

Suisun Bay is roughly 25 kilometers (km) long, has a surface area of approximately 94 square kilometers ($km^2$), a mean depth of 4.3 meters (m), and bottom topography characterized by a network of deep channels separated by a series of islands. The channels are bounded to the north and east by two large shallow regions, known as Grizzly and Honker Bays (fig. 2), that are thought to play an important role in maintaining salinities throughout the northern reach during late summer through early winter (Fischer, 1976).

### Tides

Because of its complex bathymetry and brackish water, the hydrodynamics of Suisun Bay are among the most complicated in San Francisco Bay (Walters and Gartner, 1985). The tides propagate through the channels of Suisun Bay as progressive waves where the water level and tidal currents are roughly in phase. For example, at Station BULLS (fig. 2), the currents lead the phase of the water level by about 10 minutes (harmonic analysis results, appen. C). That is, the currents reach their peak ebb/flood magnitudes roughly 10 minutes before low/high water, respectively. The currents leading the water level are typical of frictionally dominated systems such as San Francisco Bay (Officer, 1976). However, the tidal signal in the vicinity of the shallows of Grizzly and Honker Bays is more like a standing wave, due to friction and shoreline reflection (Burau and Cheng, 1988). In a pure standing wave, the water level and currents are 90 degrees out of phase. One expects standing wave behavior when the resonant frequency of an enclosed basin closely approximates the frequency of the tidal forcing. The resonant period of Grizzly and Honker Bays are on the order of $T_{res}$ ~ 1 hour, where the resonant period,

$$T_{res} \sim \frac{4L}{\sqrt{gH}},$$

is estimated by a quarter wave resonator ($g$ ~9.81m/$s^2$ is gravity and $H$ is depth; $H$ is taken to be ~1.5 m, $L$ is the length of the basin, which, for Grizzly and Honker Bays is taken to be $L$ ~4 km) (Pond and Pickard, 1983). Because the resonant periods for Grizzly and Honker Bays are much shorter (~1 hour) than the period of the tidal forcing (~12 hours), one expects only partial standing wave behavior in these small sub-bays. This is confirmed at Station GC (fig. 2) where the water level and currents are approximately 35 degrees out of phase (harmonic analysis results, appen. I). The phase relation between the water level and currents is important in the transport of salt, sediment, and biota in tidally dominated systems. Stokes drift is an upstream residual current that can occur in progressive wave systems like San Francisco Bay's northern reach (Burau and others, 1998). Stokes drift, which can be large when the water level and tidal currents are roughly in phase, can contribute significantly to transport into and out of shallow regions, such as Grizzly and Honker Bays, because the tidal range is a significant fraction of the mean depth.

### Currents

Owing to Suisun Bay's complex bathymetry, the timing, magnitude, and direction of the tidal currents vary significantly throughout Suisun Bay. An example of the spatial variability of the currents generated by a numerical model is shown in figure 3. The magnitude of tidal currents usually vary in direct proportion to the water depth (slower in the shoals); orientation is generally directed parallel to the prevailing bathymetry contours (Cheng and Gartner, 1984b). The tidal currents in the channels are on the order of 100 centimeters per second (cm/s) whereas the tidal currents in the shallows are on the order of 50 cm/s or less.

As compared to the tidal currents, the residual (tidally averaged) currents usually are an order of magnitude smaller (for example, ~10 cm/s in the channels). These residual currents are affected by Delta outflow (hydrology) and atmospheric forcing (meteorological). At times, these factors have a significant influence on the residual circulation patterns (Walters and Gartner, 1985). Therefore, the hydrologic and meteorological conditions during the study period are discussed in the following sections.

### Hydrologic Conditions

The Sacramento–San Joaquin Delta provides most of the freshwater that flows into Suisun Bay (Jassby and others, 1995). In winter and spring, this freshwater input can significantly alter the tidal and residual circulation in Suisun Bay. For example, the residual currents that are typically on the order of 10 cm/s during summer can increase to more than 60 cm/s from the influx of freshwater during uncontrolled runoff events in winter. Moreover, freshwater flows in winter or early spring can advect salt seaward of Suisun Bay, effectively removing density-driven circulation from this area during these events.

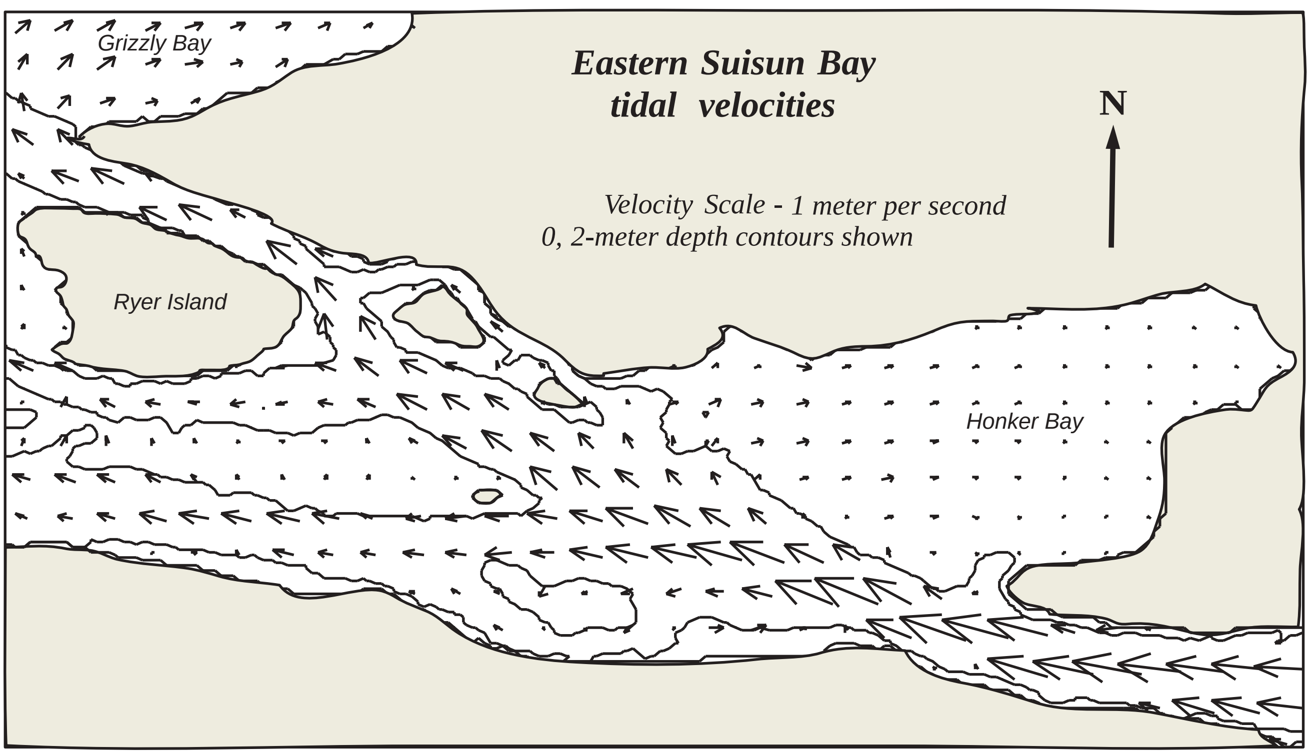


Schematic not to scale

**Figure 3.** Numerical model simulation of depth-averaged tidal current velocities in Suisun Bay, California, during ebb current (Cheng and others, 1993).

Compared to the 1993 and 1994 water years, the 1995 water year was characterized by high flows with three distinct discharge peaks in excess of 5,000 cubic meters per second ($m^3/s$) (fig. 4). The relatively high Delta outflows “pushed” salinity seaward of Suisun Bay beginning about Julian day 70. Salinity returned to the western part of Suisun Bay at Bulls Head around Julian day 145. Figure 4*D* provides a detailed time series of the Delta outflow that entered Suisun Bay during the study period. This record shows the effect on Delta outflow caused by the gate failure at Folsom Dam on the American River.

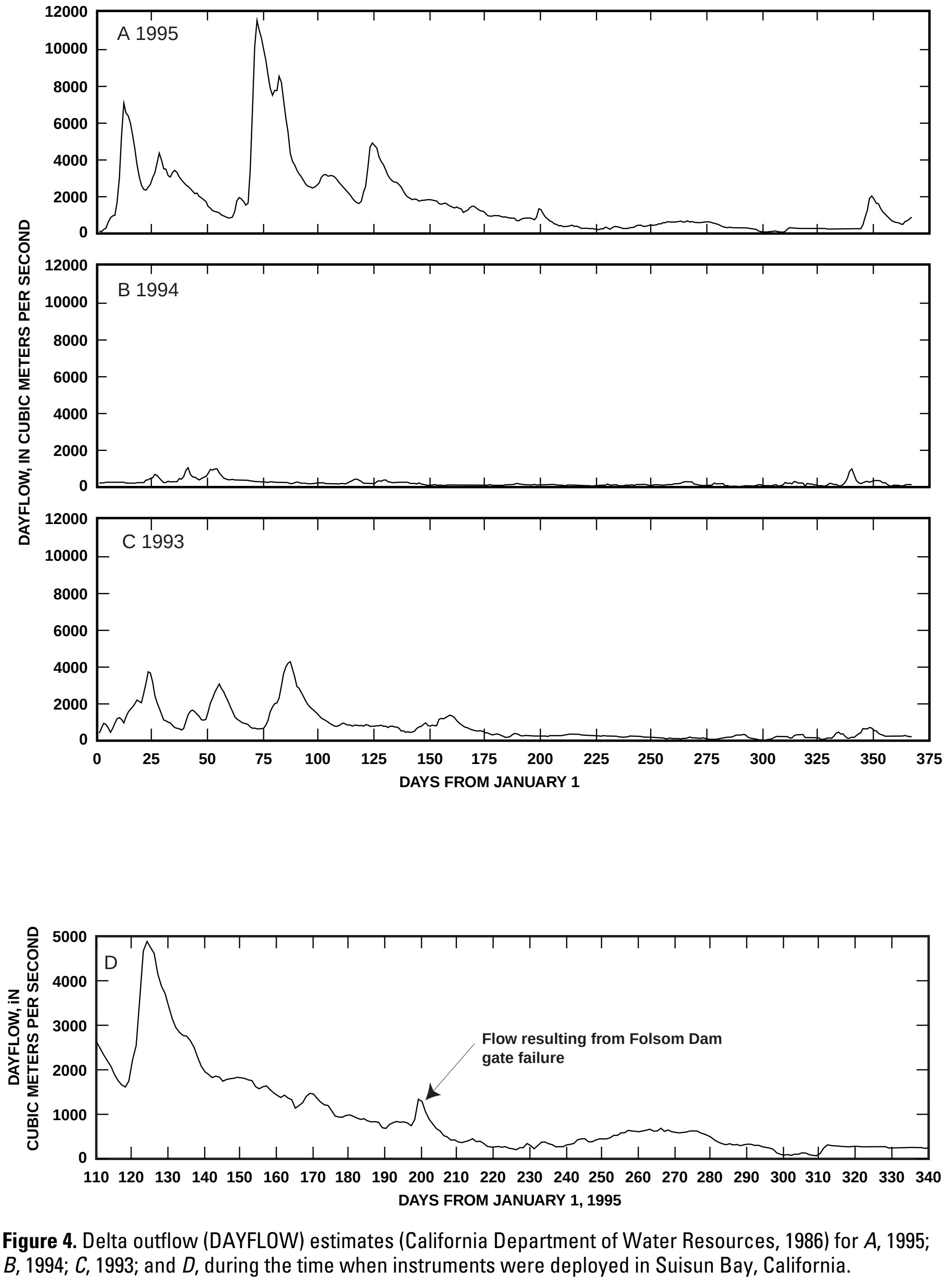


**Figure 4.** Delta outflow (DAYFLOW) estimates (California Department of Water Resources, 1986) for *A*, 1995; *B*, 1994; *C*, 1993; and *D*, during the time when instruments were deployed in Suisun Bay, California.

### Meteorological Conditions

Changes in meteorology also can affect the hydrodynamics of Suisun Bay through changes in atmospheric pressure and wind. For example, atmospheric pressure can create residual currents in Suisun Bay by significantly raising or lowering sea level (Walters and Gartner, 1985). Figure 5 shows barometric pressure, wind direction, wind speed, air temperature, and visible light measured during the study at Station Channel Marker 27 in Suisun Bay (fig. 2). Based on data shown in figure 5, the

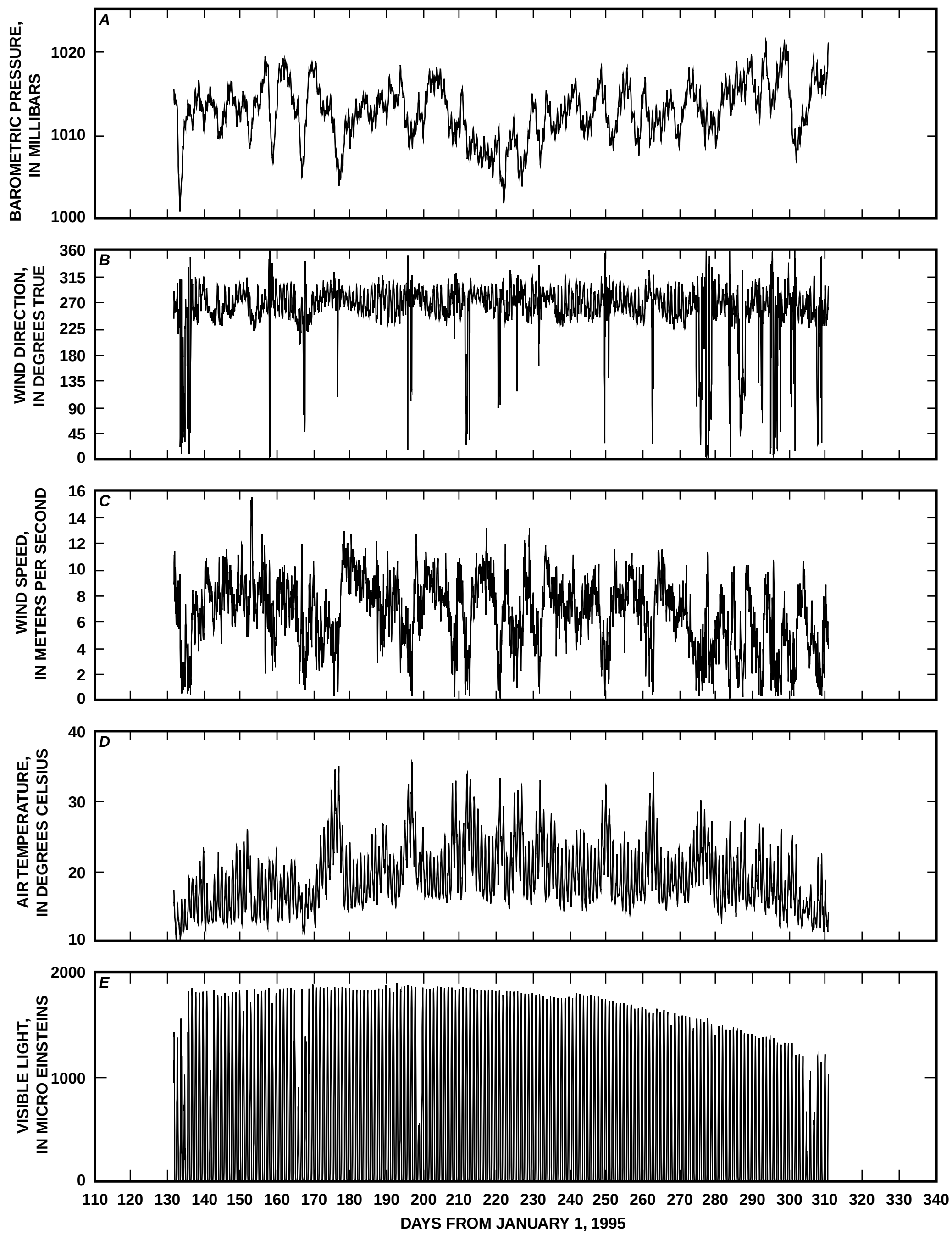


**Figure 5.** *A*, barometric pressure; *B*, wind direction; *C*, wind speed; *D*, air temperature; and *E*, visible light at Station Channel Marker 27 in Suisun Bay, California, May 12, 1995, through November 6, 1995. By convention, wind direction is reported as the direction the wind is coming from (for example, westerly winds have a direction of 270 degrees).

meteorological conditions during the 1995 study were characterized by relatively constant barometric pressures and intermittent westerly winds that varied from 0–10 meters per second (m/s). Wind stress on the water surface can produce a current that flows in the direction of the wind at the surface and flows opposite the wind direction at depth in the channels (Fischer and others, 1979; Hunter and Hearn, 1987). Wind direction is reported as the direction from which the wind is coming (westerly winds have a direction of 270 degrees). Winds in Suisun Bay are characterized by prevailing westerly and southwesterly winds in late spring, summer, and early autumn and by more intermittent southerly winds in winter (Gartner and Cheng, 1983).

### Sediment

Sediments are an important component of the San Francisco Bay estuarine system. Bottom sediments provide habitat for benthic organisms and are a reservoir of nutrients that contribute to the maintenance of estuarine productivity (Hammond and others, 1985). Potentially toxic substances, such as metals and pesticides, adsorb to sediment particles (Kuwabara and others, 1989; Domagalski and Kuivila, 1993; Flegal and others, 1996). Benthic organisms can ingest these substances and introduce them into the food web (Luoma and others, 1985; Brown and Luoma, 1995; Luoma, 1996).

The transport and fate of suspended sediments are important factors in determining the transport and fate of constituents adsorbed on the sediments. In Suisun Bay, the maximum concentration of suspended sediment usually marks the position of the turbidity maximum, which is a crucial ecological region in which suspended sediments, nutrients, phytoplankton, zooplankton, larvae, and juvenile fish accumulate (Peterson and others, 1975; Arthur and Ball, 1979; Kimmerer, 1992; Jassby and Powell, 1994; Schoellhamer and Burau, 1998; Schoellhamer 2001).

Suspended sediments limit the availability of light in San Francisco Bay, which, in turn, limits photosynthesis and primary photosynthetic carbon production (Cole and Cloern, 1987; Cloern, 1987, 1996). Suspended sediments also deposit in ports and shipping channels, which then must be dredged to maintain navigation (U.S. Environmental Protection Agency, 1992). Large tidal velocities, spring tides, and wind waves in shallow water all are capable of resuspending bottom sediments (Powell and others, 1989; Schoellhamer, 1996).

Discharge from the Delta contains 83–86 percent of the fluvial sediments that enter San Francisco Bay (Porterfield, 1980). Bottom sediments in Suisun Bay are composed mostly of silts and clays in shallow water and silts and sands in deeper water (Conomos and Peterson, 1977). An annual cycle of deposition and resuspension begins with large influx of sediment during winter, primarily from the Central Valley (Goodwin and Denton, 1991; Oltmann and others, 1999). Much of this new sediment deposits in San Pablo and Suisun Bays. Stronger westerly winds during spring and summer cause wind-wave resuspension of bottom sediment in these shallow waters and increase SSC (Ruhl and Schoellhamer, 1999). The ability of wind to increase SSC is greatest early in the spring, when unconsolidated fine sediments easily can be resuspended. As the fine sediments are winnowed from the bed, however, the remaining sediments become progressively coarser and less erodible (Conomos and Peterson, 1977; Krone, 1979; Nichols and Thompson, 1985; Ruhl and Schoellhamer, 1999).

## Acknowledgments

The authors greatly appreciate the help of Randall Brown (DWR) and Kenneth Lentz (USBR) for arranging the IEP funding for this work. The U.S. Department of Interior’s Placed Based Program provided funding for the sediment-transport component of this study and for most of the equipment used in this study. Catherine Ruhl provided the suspended-solids concentration and associated calibration plots. The authors gratefully acknowledge Paul Buchanan, Jim DeRose, Jeff Gartner, Brian McGeehan, Robert Sheipline, and Brad Sullivan of the USGS, and Mark Stacy of Stanford University for their assistance deploying, servicing, and recovering field instruments used in this study.

## FINDINGS

This report describes and documents hydrodynamic and SSC data collected in Suisun Bay from May 30 through October 27, 1995. In this section, we discuss the general spatial and temporal patterns observed in the hydrodynamic data organized by timescale, beginning with the tidal timescale and followed by the residual, or tidally averaged, timescale. The tidal and residual timescale sections include discussions on current and salinity characteristics. In addition, findings derived from the SSC data are summarized.

### Tidal Timescale Variability

#### Currents

The tidal currents often are best characterized using results from harmonic analysis. Harmonic analysis summary sheets are provided in the appendices for sea-level and tidal-current data. The spatial variability in the tidal currents are summarized in figures 6 and 7 as the spring tidal current maximum and neap tidal current minimum in vector form and the RMS current speed, numerically. Figure 6 shows the near-surface tidal currents in the channels measured using ADCPs and figure 7 shows the currents in the shallows using single-point velocity measurements. The directions of the current vectors in these figures are oriented using the principal direction of the tidal current ellipse at each location. The principal direction for each station is determined from harmonic analysis and presented in the appendices.

Figure 6 shows that the tidal currents dissipate as the tide wave propagates landward through Suisun Bay; the RMS currents are roughly 70 cm/s on Suisun Bay's western boundary compared to 60 cm/s on its eastern boundary at Mallard Island. Moreover, the RMS tidal currents are significantly less through the northern channels (~50 cm/s). Based on harmonic analysis, the magnitude of spring tidal currents are roughly twice those of the neap tidal currents. Finally, the tidal currents in the shallows are significantly less than in the channels (compare figs. 6 and 7). The tidal current ellipses in shallow regions also are less eccentric than those in channels because the currents in the shallows are less bathymetrically constrained (compare the major and minor axes of the tidal current ellipses to the harmonic analysis results for velocity in the appendices).

#### Salinity

Salinities and salinity stratification in Suisun Bay vary significantly at tidal timescales, as shown in a typical example from Suisun Cutoff, Station CUT (fig. 8). (Salinities reported here are according to the practical salinity scale and, therefore, have no units. However, sea water, which contains about 35 parts per thousand dissolved solids, is represented by 35 on the practical salinity scale.) In this example, near-bed salinities vary from 2.5 to 7 throughout the tidal cycle and salinity stratification changes from vertically well mixed (no top-to-bottom salinity difference) to significantly stratified with top-to-bottom differences on the order of 2. In advection-dominated systems such as Suisun Bay, the tidal timescale salinity variations principally are a result of the strong tidal currents and a persistent, though seasonally variable, horizontal salinity gradient typically on the order of 0.5 $km^{-1}$. In this example, salinities vary by roughly 5 throughout the tidal cycle, however the degree to which salinities vary over a tidal cycle can change depending on the strength of the horizontal salinity gradient, which itself varies at tidal, fortnightly, and seasonal timescales. For example, large changes in salinity at a fixed site are expected when the horizontal salinity gradient is locally large. Moreover, because advection dominates salt transport, salinities reach their peak at high water slack, and are lowest during low water slack, as is shown in figure 8. Finally, salinity stratification in the low salinity zone (0–10) usually is greatest during flood tides and least during ebb tides (fig. 8).

## Residual Timescale Variability

### Currents

As a typical example of velocity profiles measured in the ship channel of Suisun Bay (fig. 1), time-series of the longitudinal and transverse residual currents at Station BULLS (fig. 2) are presented in figure 9. The large vertical shears in figure 9, especially at sections A and B, show that the velocity profiles at Station BULLS are clearly affected by the presence of salinity. The example profiles given in figure 10 do not resemble a log profile typical of water surface slope-driven flows, nor do they resemble the residual current profiles typical of gravitational circulation (Hansen and Rattray, 1965). The shapes

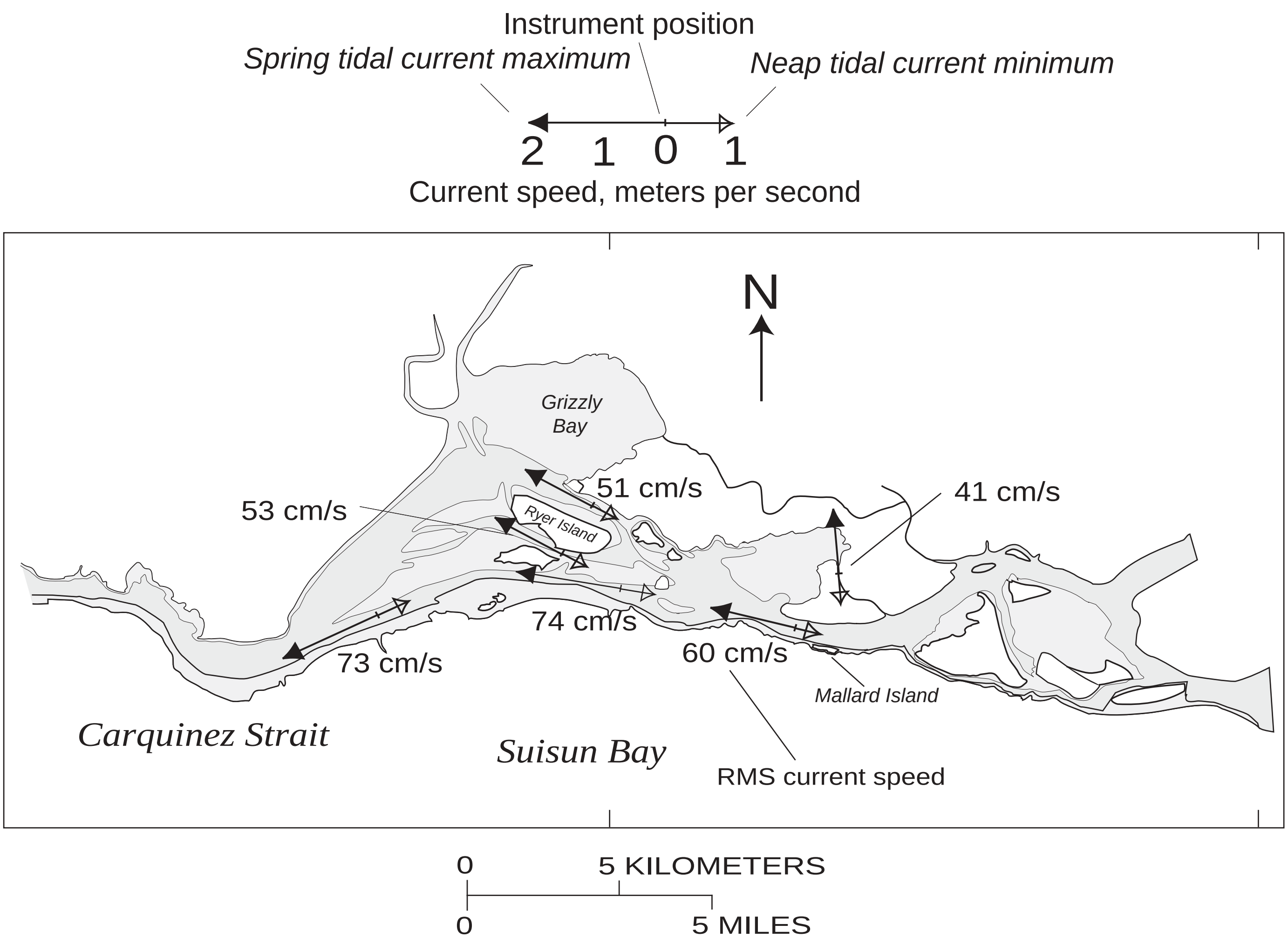


**Figure 6.** Near-surface tidal currents obtained from harmonic analysis of acoustic Doppler current profiler measurements in Suisun Bay, California, (the lengths of the vectors at each location corresponds to magnitude). The spring tidal current maximum is estimated by $(M_2 + S_2) + (O_1 + K_1)$ and the neap tidal current minimum is not less than $(M_2 - S_2) + (O_1 - K_1)$ where $M_2$ and $S_2$ are amplitudes of the principal lunar and solar semidiurnal partial tides, respectively, and $O_1$ and $K_1$ are amplitudes of the principal lunar and Luni-solar diurnal partial tides, respectively (Cheng and Gartner, 1984a). The number associated with each current vector is the root-mean-squared (RMS) current speed, in centimeters per second (cm/s).

of residual current profiles measured in Suisun Bay's ship channel are, therefore, a combination of these two archetypes.

To show that the lack of upstream near-bed Eulerian residual currents was a consistent feature throughout Suisun Bay during this study, the tidally averaged bottom currents obtained from all of the ADCPs deployed during 1995 are shown in figure 11. Positive (flood-directed) near-bed currents are indicative of gravitational circulation, which was prevalent during this study in Carquinez Straits, represented by Station BEN (fig. 11*B*, BEN). The near-bed residual currents were, for the most part, directed seaward (negative) in Suisun Bay except for a few brief periods during neap tides in Suisun Cutoff (fig. 11*C*, CUT) and for a brief period (~10 days) at the end of the record at Station MID (which also occurred during a neap tide). Since the near-bed residual currents are, for the most part, directed seaward, the residual currents cannot contribute to upstream accumulations of suspended sediment and biota, as suggested in the classic conceptual model of estuarine turbidity maxima formation (ETM) offered by Authur and Ball (1979).

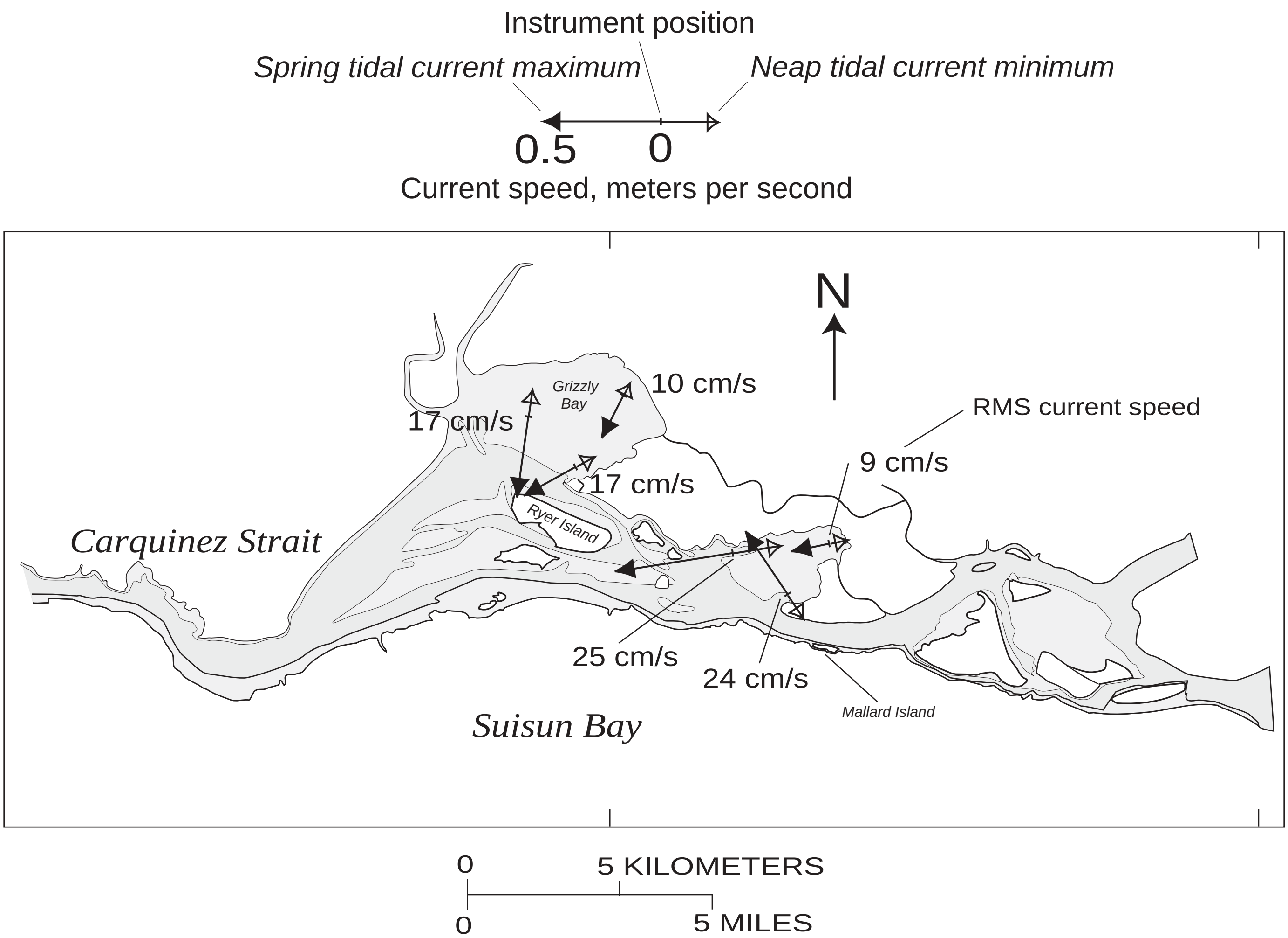


**Figure 7.** Near-bed tidal currents obtained from harmonic analysis of single-point-velocity measurements in Suisun Bay, California, (the lengths of the vectors at each location corresponds to magnitude). The spring tidal current maximum is estimated by $(M_2 + S_2) + (O_1 + K_1)$ and the neap tidal current minimum is not less than $(M_2 - S_2) + (O_1 - K_1)$ where $M_2$ and $S_2$ are amplitudes of the principal lunar and solar semidiurnal partial tides, respectively, and $O_1$ and $K_1$ are amplitudes of the principal lunar and Luni-solar diurnal partial tides, respectively (Cheng and Gartner, 1984a). The number associated with each current vector is the root-mean-squared (RMS) current speed, in centimeters per second (cm/s).

## Salinity

Subtidal salinity variability in Suisun Bay primarily depends on Delta outflow and density-driven circulation. Density-driven circulation depends on tide-induced vertical mixing which, in turn, varies with the spring/neap cycle.

Delta outflow accounts for most of the seasonal variability in salinity. During the large winter uncontrolled runoff events (fig. 4*D*) Suisun Bay can be completely fresh. At the other extreme, following

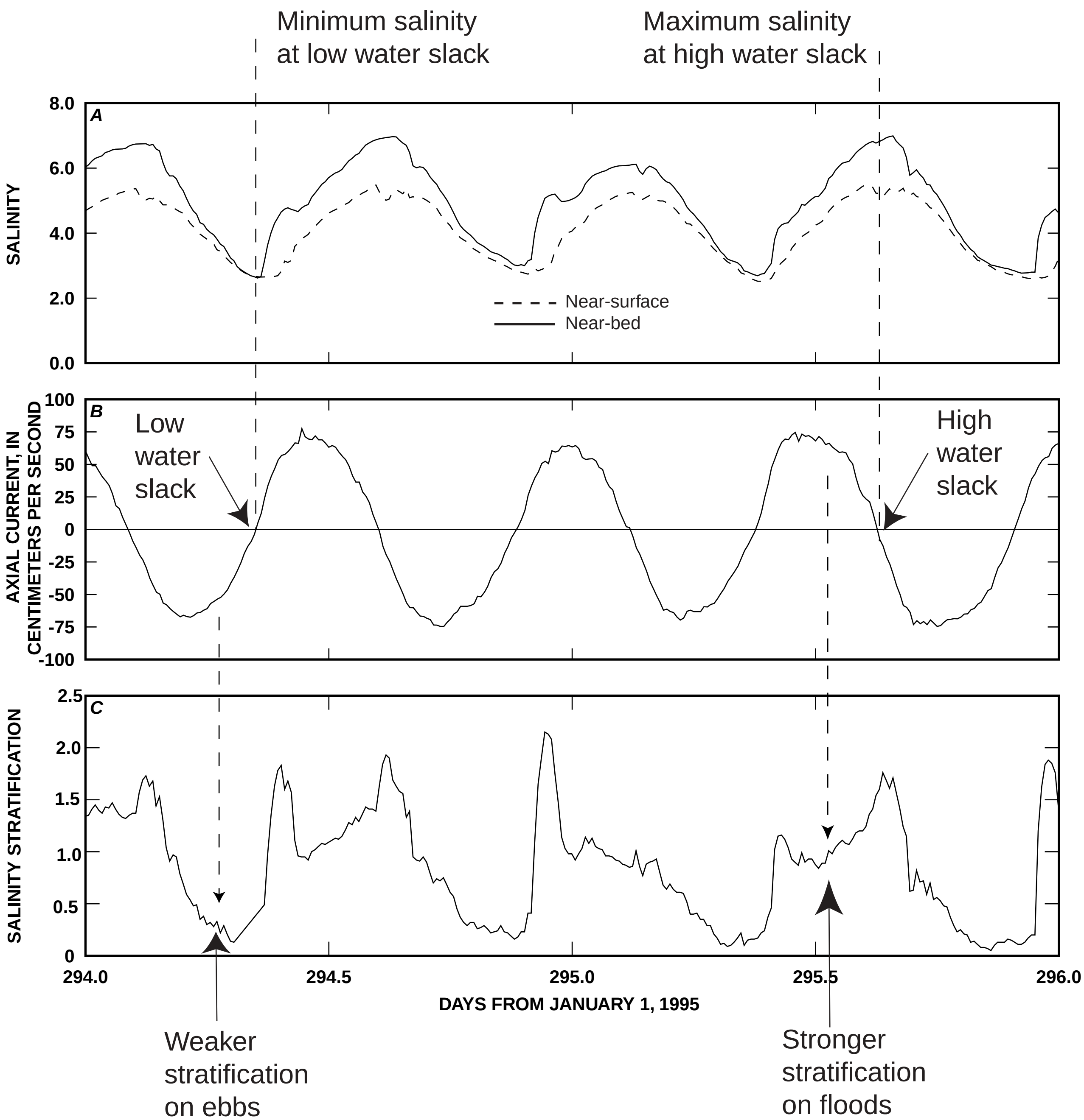


**Figure 8.** Time-series plot of *A*, salinity; *B*, depth-averaged, along-channel (axial) current speed; and *C*, vertical salinity stratification collected at Station CUT (fig. 2) in Suisun Bay, California. Salinities in this report are presented without units because salinity is a conductivity ratio function; therefore, it has no physical units (Millero, 1993).

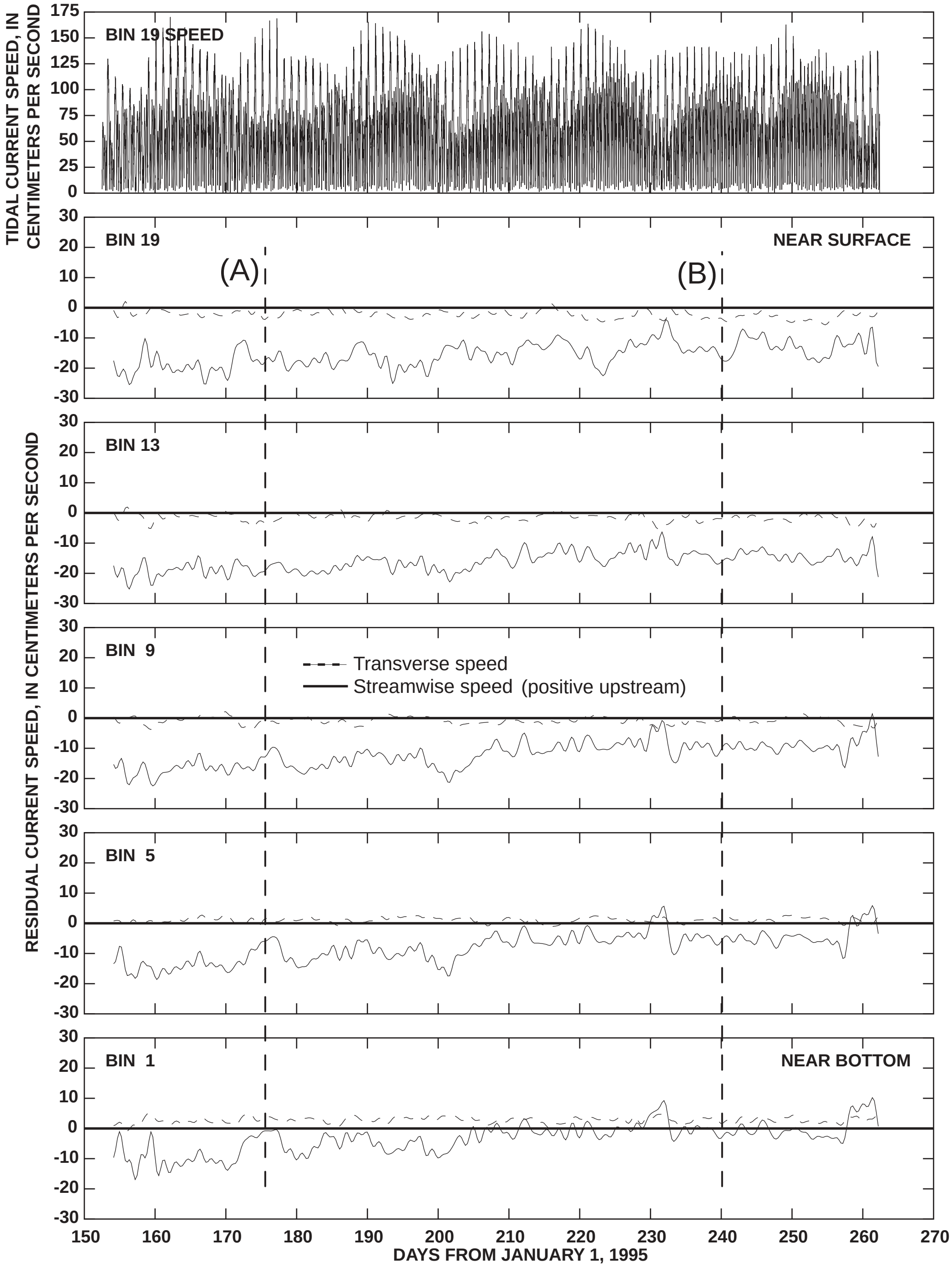


**Figure 9.** Longitudinal and transverse residual currents at Station BULLS in Suisun Bay, California, June 1, 1995, through September 19, 1995. Tidal current speed at the velocity measurement location (BIN) 19 is shown in the top panel for reference. The velocity measurement at BIN 1 is located 1.9 meters off the bed. The remaining bins are evenly spaced towards the surface at 1.0-meter intervals (BIN 2 is at 2.9 meters, etc.). Principal direction is 65.0 degrees relative to true north. (A) and (B) are presented in figure 10.

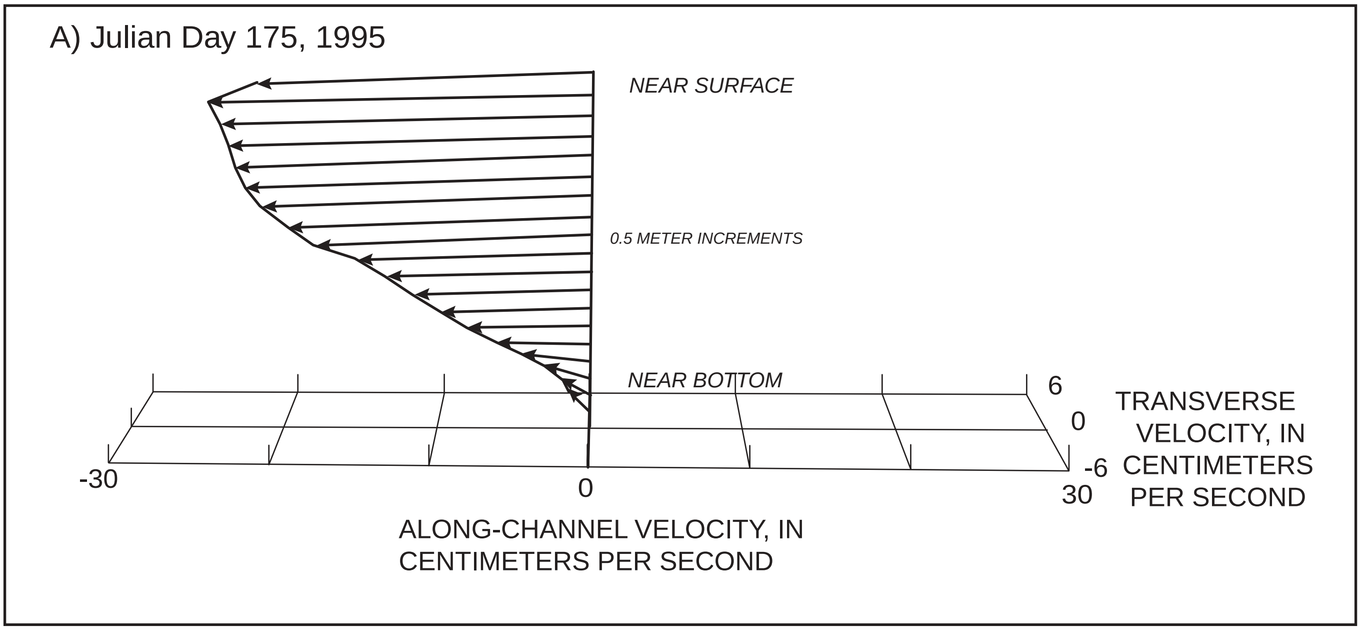


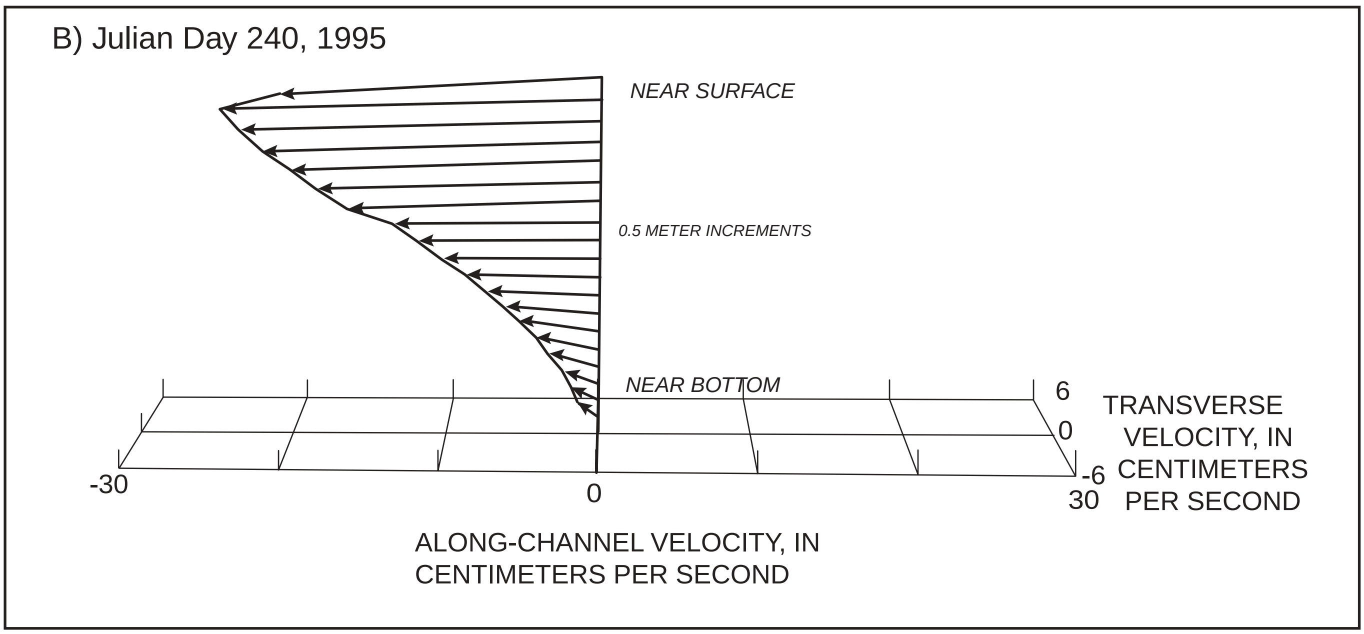


**Figure 10.** Three-dimensional perspective view of residual current profiles measured by an acoustic Doppler current profiler (Station BULLS, fig. 2) in Suisun Bay, California, on **(A)**, Julian day 175 and **(B)**, Julian day 240. These profiles were taken at the vertical dashed lines shown in figure 9. The net residual currents are down estuary in the profiles shown (though weakly so near the bed); the shear in these profiles clearly show that these profiles, nonetheless, are affected strongly by the horizontal salinity gradient. Principal direction 75 degrees.

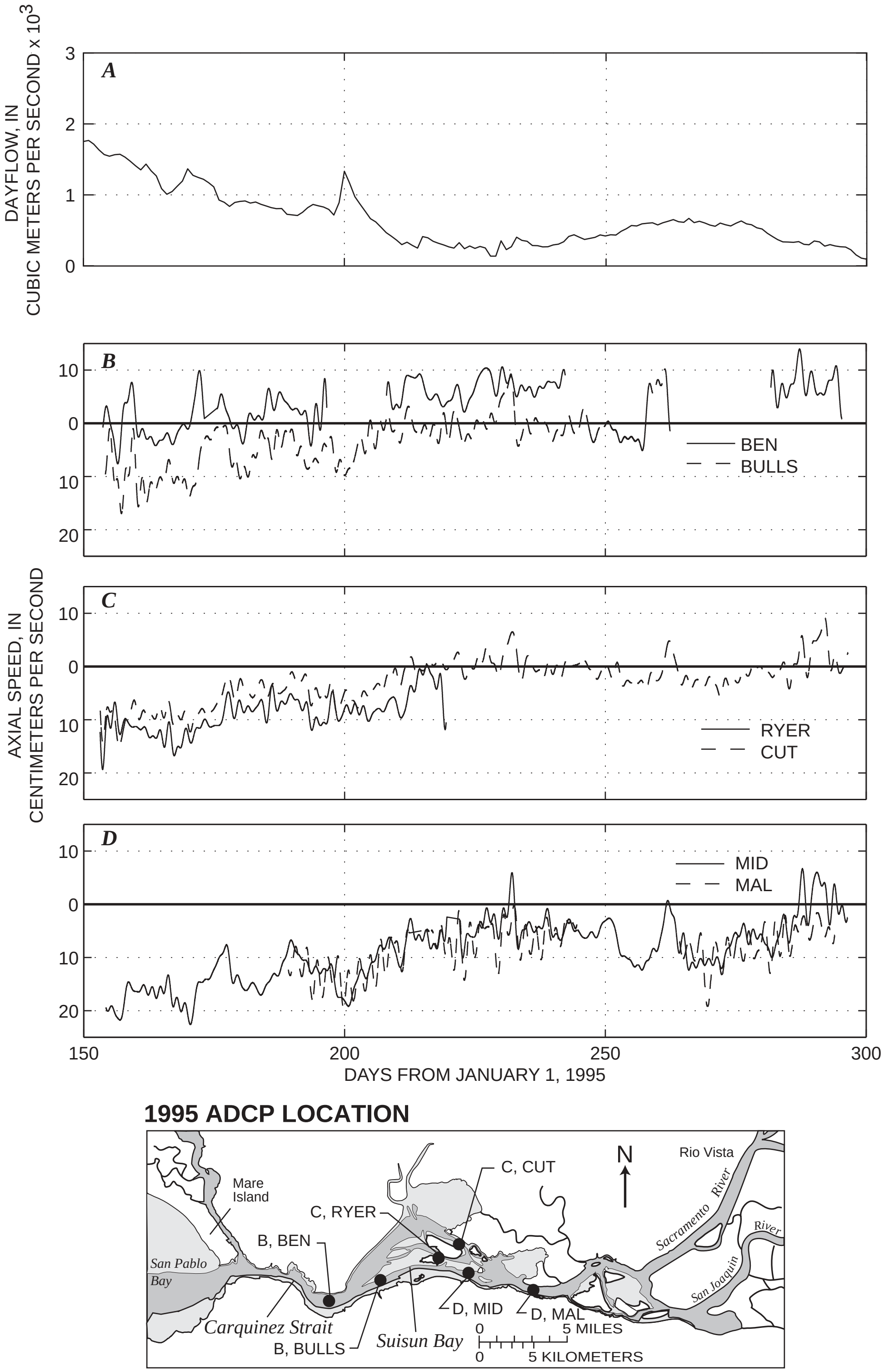


**Figure 11.** Time-series plots of *A*, DAYFLOW (California Department of Water Resources, 1986) and the near-bed residual along-channel or axial currents at *B*, Stations BEN (solid) and BULLS (dash); *C*, Stations RYER (solid) and CUT (dash); and *D*, Stations MID (solid) and MAL (dash) Suisun Bay, California, May 30, 1995, through October 27, 1995. Positive axial current speed indicates a landward flow.

periods of prolonged low Delta outflows that typically occur in late fall and early winter, salinities in Suisun Bay can be relatively high (approximately 20 at Suisun Bay's eastern end). During the study, at Station CUT, for example, the tidally filtered salinity (fig. 12*D*) varied inversely with Delta outflow (fig. 12*A*). Comparing figures 12*A* and 12*D*, one can see that as Delta outflows subsided from Julian day 200 to 235, tidally filtered salinities increased. Conversely, when Delta ouflow gradually increased from 300 to 700 $m^3$/s beginning on day 230, salinities at Station CUT decreased. And finally, when outflows began to subside again near Julian day 270, salinities began to increase.

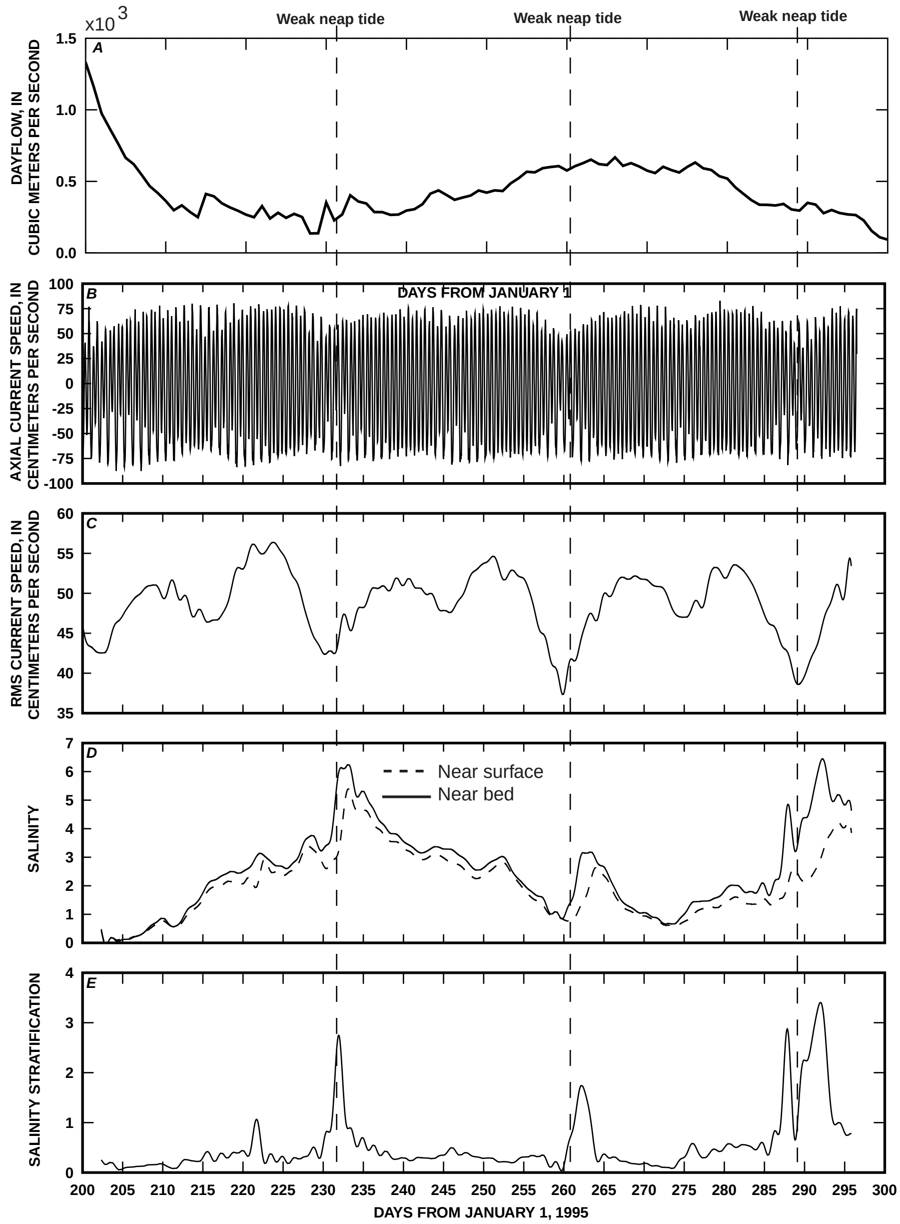


**Figure 12.** Time-series plot of Station CUT (fig. 2), Suisun Bay, California; *A*, DAYFLOW (California Department of Water Resources, 1986); *B*, depth-averaged along-channel (axial) current speed; *C*, root-mean-squared (RMS) current speed; *D*, tidally averaged near-bed (solid) and near-surface (dash) salinity; and *E*, tidally filtered vertical salinity stratification. Salinities in this report are presented without units because salinity is a conductivity ratio; therefore, it has no physical units (Millero, 1993).

At fortnightly timescales, salinity and salinity stratification varied significantly with the spring/neap cycle. Spring tides are characterized by large tidal ranges and strong tidal currents, whereas neap tides have small tidal ranges and weak current speeds. The energy in the tidal currents can be quantified by the RMS current speed that is plotted in figure 12*C*. High RMS current speeds are associated with spring tides; low RMS current speeds with neap tides. As is shown in figure 12*D*, the tidally averaged salinities episodically peak at Station CUT during weak neap tides (for example, troughs in the RMS current speed). Moreover, during neap tides, when the tidally averaged salinity is increasing, dramatic spikes in salinity stratification also occur (fig. 12*E*). Although the magnitudes of variability in the tidally averaged salinity and salinity stratification vary from site to site, these basic trends are consistently observed throughout Suisun Bay.

## Affect of Folsom Dam Spillway Gate Failure on Suisun Bay Hydrodynamics

Based on analysis of tidally averaged near-bed salinity and depth-averaged currents in the channels, the hydrodynamics of Suisun Bay were affected minimally by the Folsom Dam spillway gate failure (July 17, 1995; Julian day 198). The effect of gate failure is detectable only in Suisun Bay at the tidally averaged timescale. Even though the flows in the American River reached a peak discharge of roughly 1,000 $m^3$/s as a result of the failure, this peak is relatively small [roughly 15 percent of the approximately 7,000 $m^3$/s tidal flows that occur daily in the channels of Suisun Bay (Smith and others, 1995)] and the discharge from the failure likely was attenuated greatly when it reached Suisun Bay.

An increase in seaward (negative) flow at Mallard Island following the gate failure (fig. 13) possibly could be attributed to its occurrence. However, this increase is on the order of the longer-term natural variability in the residual currents at Mallard Island. At the stations seaward of Mallard Island [CUT (fig. 13*C*) and BULLS (fig. 13*D*)] the effect of the gate failure on the depth-averaged residual currents essentially is nonexistent. Moreover, the response of the tidally averaged near-bed salinities to the gate failure is indistinguishable from the natural variability (fig. 14). Salinity data from the eastern stations (CUT, MAL, and RYER) could not be used to assess the effect of the gate failure because these stations were completely fresh following the gate failure. Interestingly, the tidally averaged salinities at stations BULLS and MART increase slightly following the gate failure. If the gate failure had an effect, it would have lowered salinities in Suisun Bay by increasing the supply of freshwater into the eastern end of Suisun Bay. The increase in the tidally averaged near-bed salinities at these stations likely resulted from increased density driven circulation that occurred because of the neap tidal conditions during the time of the gate failure. Neap tides occur at the minima in the RMS depth-averaged current speed (fig. 14*C*).

## Sediment Transport

The hydrodynamic and SSC data have been used to study sediment transport in Honker Bay and Spoonbill Creek, salt and sediment transport in Suisun Cutoff, and an estuarine turbidity maximum (ETM) between the Reserve Fleet Channel and Suisun Cutoff. These findings are summarized below.

Warner and others (1997) determined that Spoonbill Creek at the back of Honker Bay acts as a sediment transport pathway. Significant increases in suspended-solids flux (SSF) occurred during periods of sustained winds directed along the axis of Honker Bay (westerly winds). The wind induced surface shear stress increases SSF out of Honker Bay through Spoonbill Creek through the combination of two effects: (1) wind-wave resuspension of bed sediments elevates SSC within Honker Bay, and at the same time, (2) higher water level at the eastern end of Honker Bay relative to the Sacramento River creates a net barotropic pressure gradient across Spoonbill Creek which drives a residual advective SSF from Honker Bay through Spoonbill Creek into the Sacramento River. The residual dispersive flux was also out of Honker Bay into the Sacramento River because the tidal excursion in Spoonbill Creek (approximately 4 km and approaches 6 km) is much longer than Spoonbill Creek itself (3 km). Therefore, high SSC water advected from Honker Bay into the Sacramento River through Spoonbill Creek on the ebb tide does not return on the following flood tide which creates the dispersive SSF. The total SSF was always out of Honker Bay during Fall 1995 suggesting that the relatively high metals and pesticide concentrations observed in Honker Bay are not advected through Spoonbill Creek into Honker Bay during this time of year.

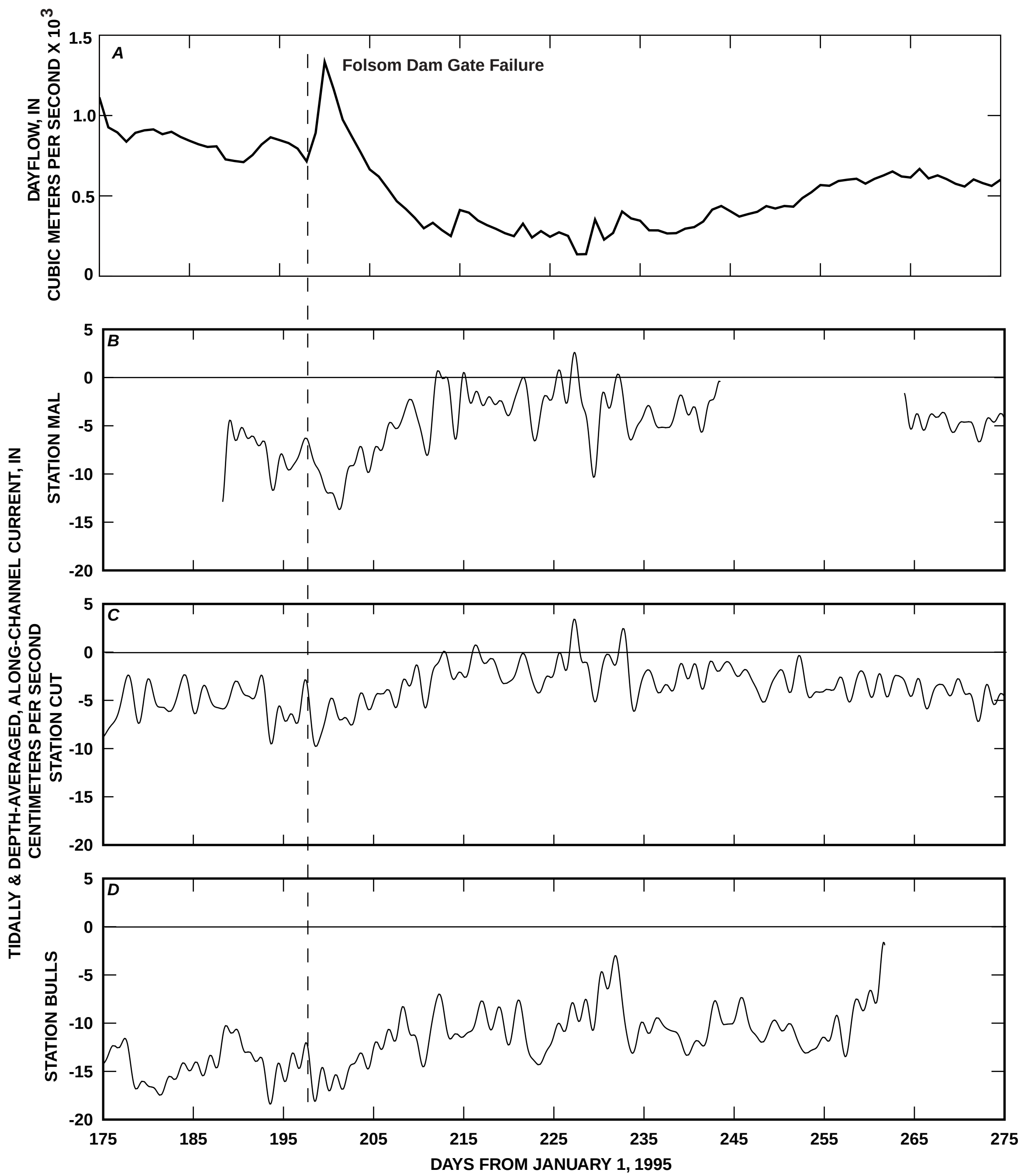


**Figure 13.** Time-series plot of *A*, DAYFLOW (California Department of Water Resources, 1986); the tidally averaged, depth-averaged, along-channel (axial) current speed at *B*, Station MAL; *C*, Station CUT; and *D*, Station BULLS (fig. 2) in Suisun Bay, California. Vertical dashed line indicates time of Folsom Dam gate failure.

Data from Suisun Cutoff shows that gravitational circulation transports salt and sediment differently (Schoellhamer and Burau, 1998). Landward pulses that develop along the bottom at the beginning of flood tides during weaker neap tides greatly increase the residual landward salt flux. SSC, however, is smallest during these neap tides and greatest during spring tides. During neap tides, when the landward pulses occur, relatively little suspended solids are available to be transported by the pulses. During spring tides, SSC is greater during floodtide than ebbtide, so the tidally-averaged flux of sediment is landward. Landward transport of sediment occurs during spring tides when gravitational circulation is weakest; thus, gravitational circulation does not necessarily cause "entrapment" in Suisun Bay.

Bottom topography enhances salinity stratification, gravitational circulation, and ETM formation seaward of sills (Jay and Musiak, 1994; Schoellhamer, 2001). The sill between the Reserve Fleet Channel and Suisun Cutoff supports the formation of an ETM (Schoellhamer, 2001). Two topographic features that place an upstream limit on gravitational circulation at the sill are a decrease in MLLW depth from 9–5 m in the landward direction at the sill and constriction of the channel in Suisun Cutoff (Burau

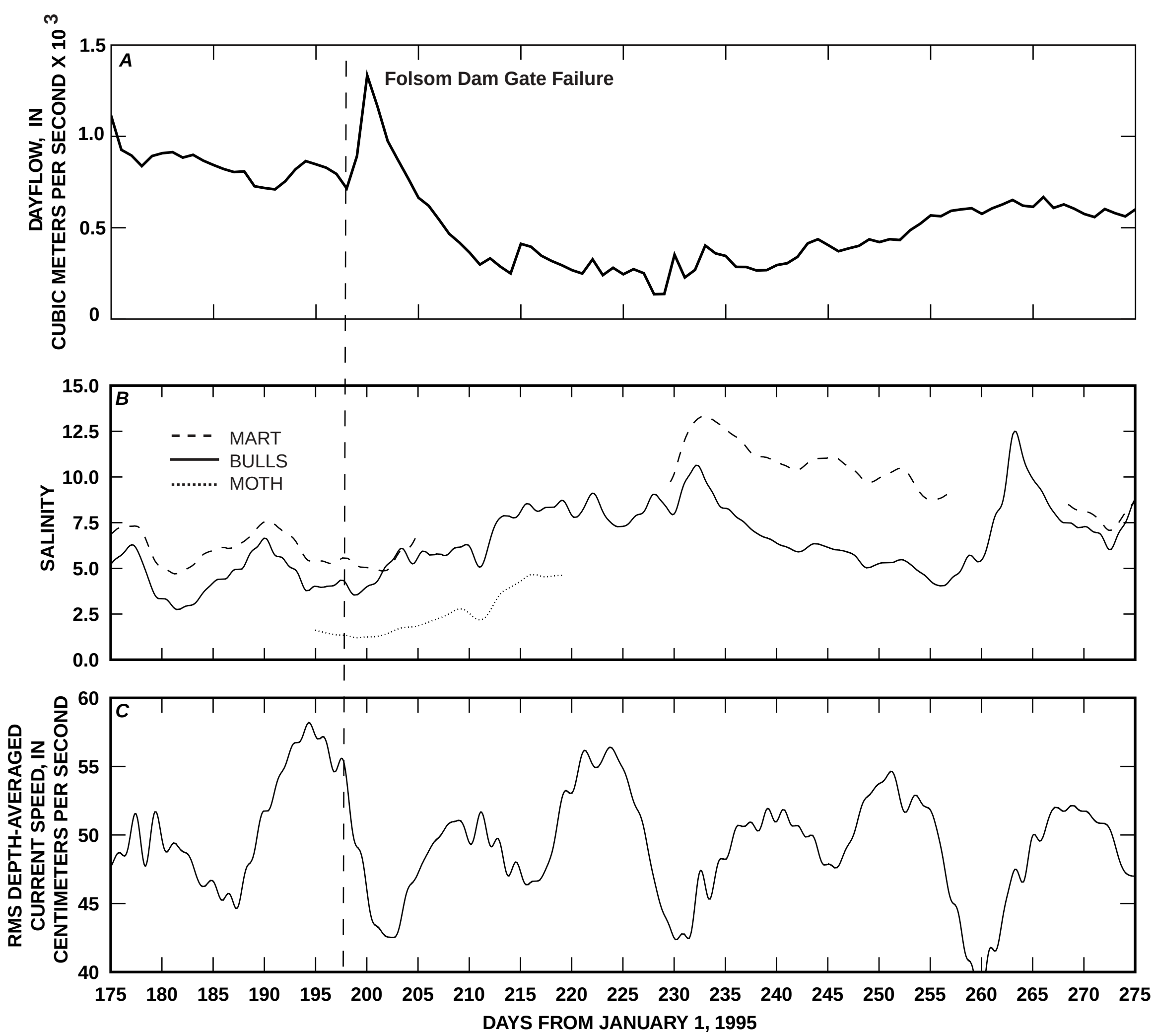


**Figure 14.** Time-series plot of *A*, DAYFLOW (California Department of Water Resources, 1986); *B*, tidally averaged salinity at Stations BULLS (solid), MART (dash) and MOTH (dot); and *C*, root-mean-squared (RMS) depth-average current speed (fig. 2) in Suisun Bay, California. Vertical dashed line indicates time of gate failure. Salinities in this report are presented without units because salinity is a conductivity ratio; therefore, it has no physical units (Millero, 1993).

and others, 1998). This topographic control traps particles in the Reserve Fleet Channel. Tidally averaged SSC always was greater in the Reserve Fleet Channel than in Suisun Cutoff as salinity returned to Suisun Bay in 1995.

## SUMMARY

Hydrodynamic and suspended-solids concentration measurements were made by the U.S. Geological Survey in Suisun Bay, California, between May 30, 1995, and October 27, 1995. The data are presented in time-series form where the tidal timescale characteristics are reflected in raw data plots and in harmonic analysis results. The tidally averaged variations in the data are captured in plots of the low-pass filtered data. These data document a period of transition from a freshwater-inflow-dominated condition towards a quasi steady-state summer condition when density-driven circulation and tidal nonlinearities become relatively important as long-term transport mechanisms. Even though salinities increased overall in Suisun Bay during the study period, the near-bed residual currents were directed primarily seaward, indicating that salinity intrusion was accomplished in the absence of gravitational circulation.

During this study, the Folsom Dam spillway failed, allowing the analysis of the hydrodynamic effects in Suisun Bay. Based on the tidally averaged near-bed salinity and depth-averaged currents after the failure, the effect was essentially nonexistent and was indistinguishable from the natural variability.

## REFERENCES CITED

Arthur, J.F., and Ball, M.D., 1979, Factors influencing the entrapment of suspended material in the San Francisco Bay–Delta Estuary, *in* Conomos, T.J., (ed.), San Francisco Bay the urbanized estuary: American Association for the Advancement of Science, p. 143–174.

Brown, C.L., and Luoma, S.N., 1995, Use of the euryhaline bivalve Potamocorbula amurensis as a biosentinal species to assess trace metal contamination in San Francisco Bay: Marine Ecology Progress Series, v. 124, p. 129–142.

Buchanan, P.A., and Schoellhamer, D.H., 1996, Summary of suspended-solids concentration data, San Francisco Bay, California, water year 1995: U.S. Geological Survey Open-File Report 96-591, 40 p.

———, 1998, Summary of suspended-solids concentration data, San Francisco Bay, California, water year 1996: U.S. Geological Survey Open-File Report 98-175, 59 p.

Buchanan, P.A., and Ruhl, C.A., 2000, Summary of suspended-solids concentration data, San Francisco Bay, California, water year 1998, U.S. Geological Survey Open-File Report 00-88.

Burau, J.R., and Cheng, R.T., 1988, Predicting tidal currents in San Francisco Bay using a spectral model: 1988 National Conference on Hydraulic Engineering, American Society of Civil Engineers, Colorado Springs, Colorado, August 8–12, 1988, Proceedings, p. 634–639.

Burau, J.R., Gartner, J.W., and Stacey, M.T., 1998, Results from the hydrodynamic element of the 1994 entrapment zone study, Suisun Bay, California, chap. 2 *in* Kimmerer, W.J., (ed.), Report of the 1994 entrapment zone study: Interagency Ecological Program for the San Francisco Bay/Delta, Technical Report 56, p. 13–62.

Burau, J.R., Simpson, M.R., and Cheng, R.T., 1993, Tidal and residual currents measured by an acoustic Doppler current profiler at the west end of Carquinez Strait, San Francisco Bay, California, March to November 1988: U.S. Geological Survey Water-Resources Investigations Report 92-4064, 76 p.

Burau, J. R., Gartner, J. W., and Stacey, M.T., 1998, Results from the hydrodynamic element of the 1994 entrapment zone study in Suisun Bay, *in* Kimmerer, W. J., (ed.), Report of the 1994 entrapment zone study. Interagency Ecological Program for the San Francisco Bay/Delta Estuary, Technical Report 56, 55 p.

California Department of Water Resources, 1986, DAYFLOW Program Documentation and DAYFLOW Data Summary User's Guide.

Cheng, R.T., Casulli, Vincenzo, and Gartner, J.W., 1993, Tidal, residual, intertidal mudflat (TRIM) model and its applications to San Francisco Bay, California: Estuarine, Coastal and Shelf Science, v. 36, p. 235–280.

Cheng, R.T., and Gartner, J.W., 1984a, Tides, tidal and residual currents in San Francisco Bay, California—results of measurements in Suisun Bay Region, , Part 1: U.S. Geological Survey Water-Resources Investigations Report 84-4339, 72 p.

Cheng, R.T., and Gartner, J.W., 1984b, Tides, tidal and residual currents in San Francisco Bay, California—results of measurements in Suisun Bay Region, Part 2: U.S. Geological Survey Water-Resources Investigations Report 84-4339, 231 p.

———, 1985, Harmonic analysis of tides and tidal currents in South San Francisco Bay, California: Estuarine, Coastal and Shelf Science, v. 21, p. 57–74.

Chereskin, T.K., Firing, Eric, and Gast, J.A., 1989, On identifying and screening filter skew and noise bias in acoustic Doppler current profiler instruments: Journal of Atmospheric and Oceanic Technology, v. 6, p. 1040–1054.

Cloern, J.E., 1987, Turbidity as a control on phytoplankton biomass and productivity in estuaries: Continental Shelf Research, v. 7, no. 11/12, p. 1367–1381.

———, 1996, Phytoplankton bloom dynamics in coastal ecosystems: a review with some general lessons from sustained investigation of San Francisco Bay, California: Reviews of Geophysics, v. 34, no. 2, p. 127–168.

Cloern, J.E., and Jassby, A.D., 1995, Year-to-year fluctuation of the spring phytoplankton bloom in South San Francisco Bay: An example of ecological variability at the land-sea interface, *in* Powell, T.M., and Steele, J.H., (eds.), Ecological Time Series: Chapman Hall, p. 139–149.

Cloern, J.E., Luoma, S.N., and Nichols, F.H., 1995, The United States Geological Survey San Francisco Bay Program - Lessons learned for managing coastal water resourced: U.S. Geological Survey Fact Sheet FS-053-95, 3 p.

Cole, B.E., and Cloern, J.E., 1987, An empirical model for estimating phytoplankton productivity in estuaries: Marine Ecology Progress Series, v. 36, p. 299–305.

Conomos, T.J., and Peterson, D.H., 1977, Suspended-particle transport and circulation in San Francisco Bay, an overview: New York, Academic Press, Estuarine Processes, v. 2, p. 82–97.

Defant, Albert, 1958, Ebb and Flow: Ann Harbor, Michigan, Ann Arbor Science Paperbacks, 121 p.

Domagalski, J.L., and Kuivila, K.M., 1993, Distributions of pesticides and organic contaminants between water and suspended sediment, San Francisco Bay, California: Estuaries, v. 16, no. 3A, p. 416–426.

Fischer, H.B., 1976, Mixing and dispersion in estuaries: Annual review of fluid mechanics, v.8, p.107–133.

Fischer, H.B., List, E.J., Imberger, J., and Brooks, N.H., 1979, Mixing in inland and coastal waters: New York, Academic Press, 482 p.

Fishman, M.J., and Friedman, L.C., 1989, Methods for determination of inorganic substances in water and fluvial sediments: U.S. Geological Survey Techniques of Water-Resources Investigations, book 5, chap. A1, 545 p.

Flegal, A.R., Rivera-Duarte, I., Ritson, P.I., Scelfo, G.M., Smith, G.J., Gordon, M.R., and Sanudo-Wilhelmy, S.A., 1996, Metal contamination *in* San Francisco Bay waters: Historic perturbations, contemporary concentrations, and future considerations: San Francisco Bay: The Ecosystem, Hollibaugh, J.T. (ed.), Pacific Division of the American Association for the Advancement of Science, San Francisco, p. 173–188.

Foreman, M.G.G., 1977 (1979), Manual for tidal heights analysis and prediction: Patricia Bay: Institute of Ocean Sciences Pacific Marine Science Report 77-10, 101 p.

Gartner, J.W., and Cheng, R.T., 1983, Observations from remote weather stations in San Francisco Bay, California, 1979–1981: U.S. Geological Survey Open-File Report 83-269, 120 p.

Goodwin, P., and Denton, R.A., 1991, Seasonal influences on the sediment transport characteristics of the Sacramento River: Proceedings of the Institute of Civil Engineers, Part 2, v. 91, p. 163–172.

Hammond, D.E., Fuller, C., Harmon, D., Hartman, B., Korosec, M., Miller, L.G., Rea, R., Warren, S., Berelson, W., and Hager, S.W., 1985, Benthic fluxes in San Francisco Bay: Hydrobiologia, v. 129, p. 69–90.

Hansen, D.V., and Rattray, M., 1965, Gravitational circulation in estuaries, Journal of Marine Research, v. 23, p. 104–122.

Hill, K.D., Dauphinee, T.M., and Woods, D.J., 1986, The extension of the practical salinity scale 1978 to low salinities: Institute of Electrical and Electronics Engineers Journal of Oceanic Engineering, v. OE-11, no. 1, p. 109–112.

Hunter, J.R., and Hearn, C.J., 1987, Lateral and vertical variations in the wind-driven circulation in long, shallow lakes: Journal of Geophysical Research, v. 92, no. 12, p. 106–114.

Jassby, A.D., and Powell, T.M., 1994, Hydrodynamic influences on interannual chlorophyll variability in an estuary: Upper San Francisco Bay–Delta (California, USA): Estuarine, Coastal and Shelf Science, v. 39, p. 595–618.

Jassby, A.D., Kimmerer, W.J., Monismith, S.G., Armor, Charles, Cleorn, J.E., Powell, T.M., Schubel, J.R., and Vendlinski, T.J., 1995, Isohaline position as a habitat indicator for estuarine populations: Ecological Applications, v. 5, no. 1, p. 272–289.

Jay, D.A., and Musiak, J.D., 1994, Particle trapping in estuarine tidal flows: Journal of Geophysical Research, v. 99, no. C10, p. 20445–20461.

Kimmerer, Wim, 1992, An evaluation of existing data in the entrapment zone of the San Francisco Bay Estuary: Tiburon, California, Biosystems Analysis, Inc., Technical Report 33, 49 p.

Kimmerer, W.J., 1998, Tidally oriented vertical migration and position maintenance of zooplankton in Northern San Francisco Bay, *in* Kimmerer, W.J. (ed.), Report of the 1994 entrapment zone study: Interagency Ecological Program for the San Francisco Bay/Delta Estuary, Technical Report 56, p. 83–111.

Kjerfve, B., 1979, Measurement and analysis of water current, temperature, salinity and density, *in* Dyer, K.R., (ed.), Estuarine hydrography and sedimentation: Cambridge, England, Cambridge University Press, p. 186–216.

Krone, R.B., 1979. Sedimentation in the San Francisco Bay system, in Conomos, T.J., (ed.), San Francisco Bay: The urbanized estuary: San Francisco, Pacific Division of the American Association for the Advancement of Science, p. 347–385.

Kuivila, K.M., and Foe, C.G., 1995, Concentrations, transport, and biological effects of dormant spray pesticides in the San Francisco Estuary, California: Environmental Toxicology and Chemistry, v. 14, no. 7, p. 1141–1150.

Kuwabara, J.S., Chang, C.C.Y., Cloern, J.E., Fries, T.L., Davis, J.A., and Luoma, S.N., 1989, Trace metal associations in the water column of South San Francisco Bay, California: Estuarine, Coastal and Shelf Science, v. 28, p. 307–325.

Luoma, S.N., 1996, The developing framework of marine ecotoxicology: Pollutants as a variable in marine ecosystems?: Journal of experimental marine biology and ecology, v. 200, p. 29–55.

Luoma, S.N., Cain, D., and Johansson, C., 1985, Temporal fluctuations of silver, copper, and zinc in the bivalve Macoma balthica at five stations in South San Francisco Bay: Hydrobiologia, v. 129, p. 109–120.

Luoma, S.N., Cain, D.J., Brown, C., and Hornberger, M., 1993, Trace metals in clams (*Macoma balthica*) and sediments at the Palo Alto mudflat in South San Francisco Bay, June 1992–May 1993: U.S. Geological Survey Open-File Report 93-500, 52 p.

Miller, R.L., Bradford, W.L., and Peters, N.E., 1988, Specific conductance; theoretical considerations and application to analytical quality control: U.S. Geological Survey Water-Supply Paper 2311, 16 p.

Millero, F.J., 1993, What is a psu?: Oceanography, v. 6, no. 3, p. 67.

Nichol, G.D., 1996, Estuarine circulation cell of lower Sacramento River: Reno, University of Nevada, Ph.D. thesis, 197 p.

Nichols, F.H., and Thompson, J.K., 1985. Time scales of change in the San Francisco Bay benthos, Hydrobiologia v. 192, p. 121–138.

Nichols, F.H., Thompson, J.K., and Schemel, L.E., 1990, Remarkable invasion of San Francisco Bay (California, USA) by the Asian clam *Potamocorbula amurensis*. II. Displacement of a former community: Marine Ecology Progress Series, v. 66, p. 95–101.

Officer, C.B., 1976, Physical oceanography of estuaries (and associated coastal waters), John Wiley and Sons, New York, p. 467.

Oltmann, R.N., Schoellhamer, D.H., and Dinehart, R.L., 1999, Sediment inflow to the Sacramento–San Joaquin Delta and the San Francisco Bay: Interagency Ecological Program newsletter, v. 12, no. 1, p. 30–33.

Peterson, D.H., Conomos, T.J., Broenkow, W.W., and Doherty, P.C., 1975, Location of the non-tidal current null zone in northern San Francisco Bay: Estuarine and Coastal Marine Science, v. 3, p. 1–11.

Peterson, D., Cayan, D., DiLeo, J., Noble, M., and Dettinger, M., 1995, The role of climate in estuarine variability: American Scientist, v. 83, p. 58–67.

Pond, S., and Pickard, G.L., 1983, Introduction to dynamical oceanography, Pergamon Press, New York, p. 329

Porterfield, George, 1980, Sediment transport of streams tributary to San Francisco, San Pablo, and Suisun Bays, California, 1909–1966: U.S. Geological Survey Water-Resources Investigations Report 80-64, 91 p.

Powell, T.M., Cloern, J.E., and Huzzey, L.M., 1989, Spatial and temporal variability in South San Francisco Bay (USA). I. Horizontal distributions of salinity, suspended sediments, and phytoplankton biomass and productivity: Estuarine, Coastal and Shelf Science, v. 28, p. 583–597.

R.D. Instruments, Inc., 1989, Acoustic Doppler current profilers—principles of operation. A practical primer: San Diego, Calif., R.D. Instruments, Inc., 36 p.

Ruhl, C.A., and Schoellhamer, D.H., 1999, Time series of suspended-solids concentration in Honker Bay during water year 1997: 1997 Annual Report of the Regional Monitoring Program for Trace Substances, p. 82–92. URL: http://www.sfei.org/rmp/1997/c0304.htm

Schoellhamer, D.H., 1996, Factors affecting suspended-sediment concentrations in South San Francisco Bay, California: Journal of Geophysical Research, v. 101, no. C5, p. 12087–12095.

Schoellhamer, D.H., Cacchione, D.A., Rubin, D.M., Cheng, R.T., Dingler, J.R., Jaffe, B.E., and Stumpf, R.P., 1997, Sediment-transport research in San Francisco Bay: Proceedings of USGS Sediment Workshop, Harpers Ferry, West Virginia, February 4–7, 1997, URL: http://wwwrvares.er.usgs.gov/osw/workshop/schoellhamer.html

Schoellhamer, D.H., and Burau, J.R., 1998, Summary of findings about circulation and the estuarine turbidity maximum in Suisun Bay, California: U.S. Geological Survey Fact Sheet FS-047-98, 6 p.

Schoellhamer, D.H., 2001, Influence of salinity, bottom topography, and tides on locations of estuarine turbidity maximum in northern San Francisco Bay, *in* McAnally, W.H., and Mehta, A.J., ed., Coastal and Estuarine Fine Sediment Transport Processes: Elsevier Science B.V., p. 343–357. URL: http://ca.water.usgs.gov/abstract/sfbay/elsevier0102.pdf

Schureman, Paul, 1976, Manual of harmonic analysis and predictions of tides: U.S. Coast and Geodetic Survey Special Publication no. 98, 317 p.

Siegel, A.R., 1982, Robust regression using repeated medians: Biometrika, v. 69, p. 242–244.

Smith, P.E., Oltmann, R.N., and Smith, L.H., 1995, Summary report on the interagency hydrodynamic study of San Francisco Bay-Delta estuary, California: Interagency Ecological Program Technical Report 45, 72 p.

UNESCO, 1985, The international system of units (SI) in oceanography: Paris, France, UNESCO Technical Papers no. 45, IAPSO Pub. Sci. no. 32.

U.S. Environmental Protection Agency, 1992, State of the estuary: Dredging and waterway modification: U.S. Environmental Protection Agency San Francisco Estuary Project, chap. 8, p. 191–215.

Walters, R.A., Cheng, R.T., and Gartner, J.W., 1985, Harmonic analysis of tides and tidal currents in South San Francisco Bay, California: Estuarine, Coastal and Shelf Science, v. 21, p. 57–74.

Walters, R.A. and Gartner, J.W., 1985, Subtidal sea level and current variations in the northern reach of San Francisco Bay: Estuarine, Coastal and Shelf Science, v. 21, p. 17–32.

Walters, R.A., and Heston, Cynthia, 1982, Removing tidal-period variations from time-series data using low-pass digital filters: Journal of Physical Oceanography, v. 12, p. 112–115.

Warner, J.C., Schoellhamer, D.H., and Burau, J.R., 1997, A sediment transport pathway in the back of a nearly semienclosed subembayment of San Francisco Bay, California: Proceedings of the XXVII International Association of Hydraulic Research Congress, August 10–15, 1997, San Francisco, California, v. 2, p. 1096–1101.

**THIS PAGE INTENTIONALLY LEFT BLANK**